Challenge Journal of

# CONCRETE RESEARCH LETTERS

Vol.15 No.3 (2024)

acoustic emission aerated concrete artificial neural network compressive strength corrosion cracking ductility durability energy absorption ferrocement flexural strength fly ash fracture mechanics mechanical properties mortar nanoparticle reinforced concrete self- compacting concrete steam curing strengthening superplasticizer tensile strength workability waste disposal water a tion

ISSN 2548-0928

TULPAR
ACADEMIC PUBLISHING

Challenge Journal of Concrete Research Letters



**E-mail:** *cjcrl@challengejournal.com*

**Web page:** *cjcrl.challengejournal.com*

**Tulpar Academic Publishing**
*www.tulparpublishing.com*

Challenge Journal of Concrete Research Letters

# CONTENTS

## *Research Articles*



TULPAR ACADEMIC PUBLISHING

Challenge Journal of Concrete Research Letters

**Research Article**

# A different approach for green concrete production: Determination of the effect of e-waste and waste rubber powder on durability properties of concrete

H. Alperen Bulut [a,*]

[a] *Department of Civil Engineering, Erzincan Binali Yıldırım University, 24002 Erzincan, Türkiye*

**ABSTRACT**

This study was carried out to present a different approach to green concrete production by utilizing electronic waste (e-waste) and waste rubber powders in order to provide a solution to both the cost and carbon footprint problems arising from the rapid consumption of aggregate resources and cement. For this purpose, 0%, 5% and 10% of e-waste was utilized instead of aggregate and 0%, 2.5% and 5% of waste rubber powder was utilized instead of cement. In addition, mixtures in which both wastes were combined in concrete were also prepared and comparisons were conducted. Capillary water absorption, acid and sulfate attack tests were carried out on the concretes with different wastes at the end of 28 and 90 days. The capillary water absorption of concrete produced with 5% waste rubber powder at the end of 28 days (P5E0/28) was 80% less than the control concrete (C/28) (these values were 0.46, 2.36 respectively). It was determined that the utilization of waste rubber powder had a decreasing effect on the compressive strength losses of the concretes after acid attack compared to the control concrete, while e-waste had an increasing effect. It was determined that the compressive strength losses of the concretes in which waste rubber powder and e-waste were combined against sulfate attack were positively differentiated from both control concrete and concretes produced with single waste type. In parallel with the weight and compressive strength losses obtained after acid and sulfate attack, the results of the visual analyses of the concretes were similar. The use of 5% waste rubber powder in the concrete produced the greatest results. In addition, the ideal ratio between concretes in which e-waste and waste rubber powder used together was determined as 5% waste rubber powder and 5% e-waste. The results verified that e-waste and waste rubber powder can be considered for the production of green concrete.

**ARTICLE INFO**

*Article history:*
Received 21 February 2024
Revised 10 April 2024
Accepted 25 April 2024

*Keywords:*
Green concrete
E-waste
Waste rubber powder
Capillary water absorption
Acid attack
Sulfate attack



## 1. Introduction

As a result of the rapid advancement of technology and the unregulated disposal of electronic devices (e.g. photocopiers, computers, televisions, printers, mobile phones, white goods, etc.) that can be produced at lower costs, a new type of waste called electronic waste (e-waste) has emerged (Kiddee et al. 2013; Farooq et al. 2019). The amount of e-waste among solid wastes is increasing day by day (Bhutta et al. 2011). For example, 44.7 million tonnes of e-waste was reported worldwide in 2016 (Hameed et al. 2020). The rate of recycled e-waste is only 12.5% and the rest is either discarded or incinerated (Ullah et al. 2022). Direct disposal of e-waste, which contains composite materials in the structure, is not feasible, thus posing significant damage to both the environment and health worldwide (Partheeban et al. 2021). This situation has enabled the utilization of e-waste as a potential material in construction practices.

* *Corresponding author*. Tel.: +90-446-224-0088 ; E-mail address: habulut@erzincan.edu.tr (H. A. Bulut)
ISSN: 2548-0928 / DOI: https://doi.org/10.20528/cjcrl.2024.03.001

Studies evaluating e-waste in concrete have started to increase rapidly in the literature. For example, improvements in the abrasion resistance of e-waste concretes have been reported (Ferreira et al. 2012). As a result of the study conducted by Gawatre et al. (2015), the ideal compressive strength was obtained with the utilization of 7.5% e-waste. In another study (Suchithra et al. 2015), it was determined that concrete produced with e-waste had high resistance to chloride attack. Compressive and splitting tensile strengths decreased as a result of e-waste utilization instead of fine aggregate in concrete (Alagusankareswari et al. 2016). As a result of the evaluation of e-waste as aggregate in polymer concretes, which is a special type of concrete, it was found that e-waste increased the ductility of polymer concretes, although mechanical properties decreased as the e-waste ratio increased (Bulut and Şahin 2017). As a result of the study carried out by Ullah et al. (2022), decreases in the compressive strength of e-waste added concretes were observed with the effect of high temperature.

Overall technological developments, industrialization, urbanization, and expansion of the construction sector due to the population growth have quickly presented humankind with unprecedented problems. One significant consequence of this is the increase in the amount of waste products (Canbaz et al. 2021; Şengel et al. 2022a). Utilizing waste materials in concrete structures is crucial for environmental cleanup and recycling (Karalar and Çavuşlu 2022). Waste tires generated by the rapidly developing automobile industry have demonstrated tremendous annual growth globally (Colette et al. 2023). In fact, statistics report that the amount of waste tires generated worldwide each year exceeds 1.5 billion (Qaidi et al. 2021). It is known that waste tires, which are intended to be destroyed by traditional disposal methods (storage, incineration, burial, etc.), both lead to environmental pollution and increase carbon emissions (Islam et al. 2023a). Thus, the disposal of waste tires in an environmentally friendly and economical way has gained urgency globally (Jurado et al. 2023). In recent years, the utilization of waste tires in civil engineering practices has become widespread (Jiang et al. 2019; Gao et al. 2024).

Many studies on rubberized concretes produced with waste rubbers are present in the literature. In a study, it was reported that compressive strength losses reached 20% when 20% waste rubber was incorporated into concrete (Youssf et al. 2020). Mechanical properties, durability and deformation of rubberized concretes were investigated (Xu et al. 2021), and it was determined that chloride permeability decreased (Thomas et al. 2016), while ductility (AbdelAleem and Hassan 2022; Şengel et al. 2022b), toughness (Bahtli and Ozbay 2021) and thermal conductivity increased (Ma et al. 2023) as a result of utilizing the proper rubber particles in concrete. Kandil and Bulut (2023) investigated the behavior of concretes containing different proportions of waste rubbers against acid and sulfate attack. As a result, it was stated that rubberized concretes with a water/cement ratio of 0.5 exhibited high resistance to acid and sulfate attack. It was also emphasized that 12% and 16% waste rubber ratios are ideal ratios. In addition, as a result of a study conducted by Bulut (2024), both splitting tensile strength and UPV (Ultrasonic pulse velocity) test results gave the best results as a result of using 2.5% waste rubber and 5% e-waste rates together in concrete.

This study was carried out to present a different approach to green concrete production by evaluating electronic waste (e-waste) and waste rubber powders in order to provide a solution to both cost and carbon footprint problems arising from the rapid consumption of aggregate resources and cement. For this purpose, 0%, 5% and 10% of e-waste was substituted for aggregate and 0%, 2.5% and 5% of waste rubber powder was substituted for cement in concrete. In addition, mixtures in which both wastes were combined in concrete were also prepared and comparisons were carried out. Capillary water absorption, acid and sulfate attack experiments were carried out on concretes with different wastes after 28 and 90 days. The novelty of the research, unlike the literature, is that the durability properties of concrete are examined at both normal and advanced ages by using e-waste instead of aggregate and waste rubber powder instead of cement in different proportions in concrete production. In addition, it was aimed to increase the originality of the study by using these two waste types together and evaluating their effect on the durability performance of concrete. Thus, the effects of both types of waste on concrete will be comprehensively evaluated and introduced to the literature.

## 2. Materials and Method

### *2.1. Materials*

CEM I 42.5 R type Portland cement was employed as a binder material for concretes with different wastes. The properties of this cement are presented in Table 1. Within the scope of the study, 4/8 mm and 8/16 mm graded coarse aggregates of crushed stone origin and 0/2 mm and 2/4 mm graded natural river sand were utilized as fine aggregates. The specific gravity of coarse aggregates of crushed stone origin was 2.651 for 4/8 mm gradation and 2.675 for 8/16 mm gradation. The specific gravity of fine aggregates is 2.478. As a result of preliminary tests, aggregate grades of 0/2 = 35%, 2/4 = 20%, 4/8 = 25% and 8/16 = 20% were selected and sieve analysis was performed according to TS EN 933-1 (2012) and TS 802 (2016) standards.

Superplasticizer chemical additive material was employed in the study. Information about this material is provided in Table 2. E-waste from electronic devices such as mobile phones, printers, monitors and televisions were shredded to aggregate size in the factories of Exitcom Recycling Company (Kocaeli/TR) and substituted for crushed stone and river sand in concrete production. The specific gravity of e-waste is 1.290. The visual of e-waste is presented in Fig. 1.

Waste rubber powder, which was utilized instead of cement, was obtained from Cemer Company (İzmir/TR). The visual of the waste rubber powder is presented in Fig. 2. The grain size distribution of waste rubber powder is given in Fig. 3.

**Table 1.** Properties of CEM I 42.5 R type Portland cement.

| Chemical Compositions (%) | |
|---|---|
| $SiO_2$ | 19.27 |
| $Al_2O_3$ | 4.62 |
| $Fe_2O_3$ | 3.23 |
| CaO | 63.05 |
| MgO | 2.43 |
| $SO_3$ | 2.88 |
| $Na_2O$ | 0.32 |
| $K_2O$ | 0.70 |
| $Cl^-$ | 0.01 |
| Loss on ignition | 2.79 |
| Insoluble residue | 0.70 |
| **Physical Characteristics** | |
| Residue on a 32 micron sieve | 7.34 |
| Specific gravity | 3.10 |
| Specific surface ($cm^2/g$) | 3432 |
| Beginning of setting | 2hrs-31min |
| End of setting | 3hrs-27min |
| Volume expansion (mm) | 1.0 |
| Compressive strength (MPa) | |
| 2nd day | 27.9 |
| 28th day | 53.6 |

**Table 2.** Properties of the superplasticizer (ViscoCrete SF-18).

| | |
|---|---|
| Chemical base | Modified polycarboxylate based polymer |
| Appearance | Light brownish liquid |
| Density (at +20°C) ($gr/cm^3$) | 1.10 |
| pH value | 3-7 |
| Alkali content (w/w, %) | ≤ 3 |
| Soluble in water chloride ion content (by mass, %) | ≤ 0.10 |
| Freezing point | -10 °C |

**Fig. 1.** Image of e-wastes.

**Fig. 2.** Image of waste rubber powders.

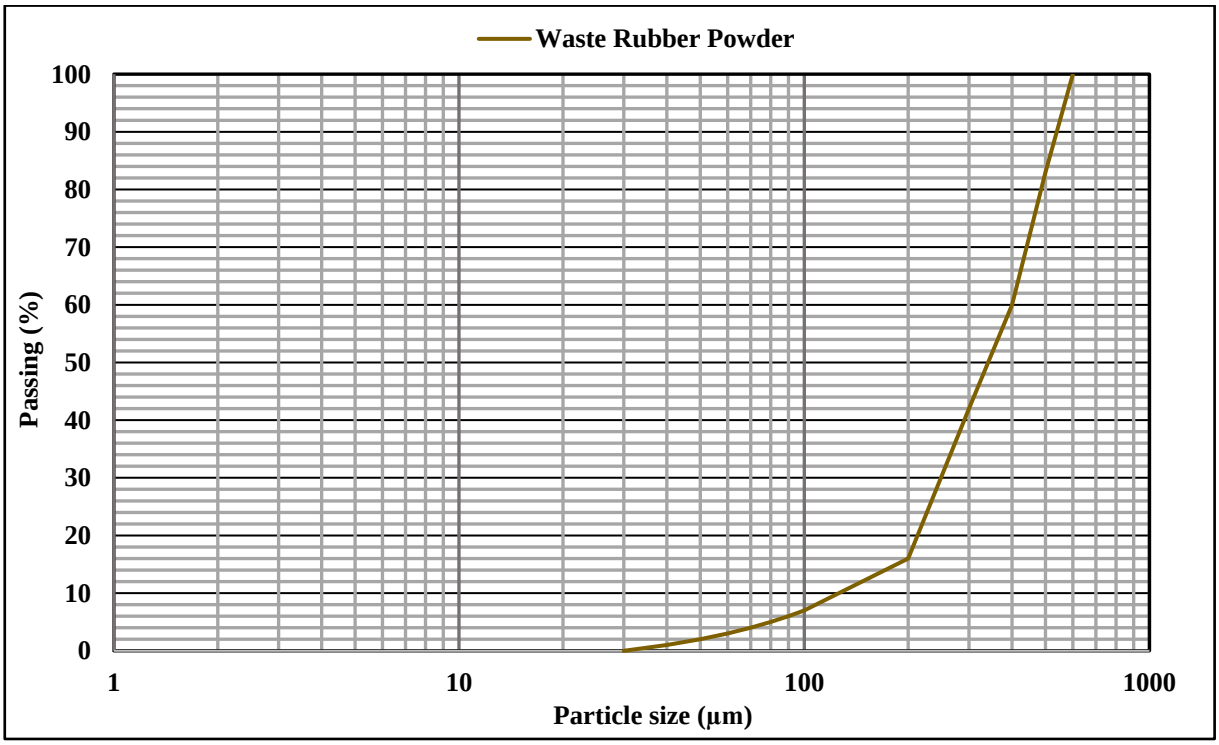


**Fig. 3.** Particle size distribution of waste rubber powder.

### *2.2. Parameters, coding and concrete mix design*

The first parameter selected in this study is the different types of wastes and their proportions. In this context, 0%, 5% and 10% e-waste was utilized instead of aggregate and 0%, 2.5% and 5% by weight of waste rubber powder was utilized instead of cement. There was no waste type in the control concretes. The second parameter of the study was the comparison of capillary water absorption, acid and sulfate attack tests, which are the durability properties of concrete, at both 28 and 90 days. It is also considered that the single and combined utilization of both waste types in concrete is also a parameter for the study.

In the coding of the concretes, the abbreviations of the waste types (in English) are indicated by letters, the ratios are indicated by numbers, and the test days are indicated by numbers after the '/' sign. For example, P2.5E10/90 represents concrete containing 2.5% waste rubber powder and 10% e-waste and tested on day 90. Control concretes are indicated by the letter C. Water/cement ratio, cement dosage and superplasticizer ratio were constant at 0.45, 400 kg/m$^3$ and 1.8% respectively.

By using new generation superplasticizer chemical additives in concrete production, the slump values of concrete could be kept constant at 8 ± 1 cm. Considering that the slump value affects both the strength and durability properties of concrete (Moustafa and ElGawady 2015; Gesoglu et al. 2017; Helmy et al. 2023), it is considered that the properties of concrete to be examined in this study can be analyzed meaningfully by keeping the slump values constant thanks to the superplasticizer. Concrete mix design is presented in Table 3. In the coding in Table 3, the numbers representing the day of the experiments were excluded.

**Table 3.** Concrete mix design (kg/m$^3$).

| Code | Cement | E-waste | Waste rubber powder | Fine agg. | Coarse agg. | Water |
|---|---|---|---|---|---|---|
| C | 400 | | | 928.09 | 815.62 | 180 |
| P2.5E0 | 390 | | 10 | 927.62 | 814.51 | 180 |
| P5E0 | 380 | | 20 | 926.49 | 813.51 | 180 |
| P0E5 | 400 | 43.92 | | 881.69 | 774.85 | 180 |
| P0E10 | 400 | 87.85 | | 835.28 | 734.07 | 180 |
| P2.5E5 | 390 | 43.92 | 10 | 871.33 | 742.38 | 180 |
| P2.5E10 | 390 | 87.85 | 10 | 834.69 | 733.51 | 180 |
| P5E5 | 380 | 43.92 | 20 | 853.22 | 724.56 | 180 |
| P5E10 | 380 | 87.85 | 20 | 822.73 | 714.43 | 180 |

### 2.3. Methods

Experiments were carried out on concretes with different ratios of e-waste and waste rubber powder at the end of 28 and 90 days curing period. In order to carry out the dry weighing ($W_0$) of the concrete in the capillary water absorption test, the samples were dried in an oven (65±5 °C) for one day and cooled at ambient temperature. The concretes were placed in 5 cm contact with water (measured by the size of their surface area ($F$, cm²), the mass increase was found by weighing the amount of water absorbed in 1-4-9-16-25-36-49-64-81 minutes ($t$, min). Capillary water absorption coefficients were calculated by the slope of the curve obtained from the square root of the amount of water absorbed from the unit area and the elapsed time. The calculated values were also confirmed by Eq. (1).

$$K = \frac{Q}{F.\sqrt{t}} \quad (1)$$

In Eq. (1), $K$; capillary water absorption coefficient, $Q$; amount of water absorption, $F$; denotes the surface area where the samples come into contact with water, and $t$ denotes the time. Capillary water absorption experiments were performed on cube samples after 28 and 90 days. Acid and sulfate tests were carried out on two samples from each concrete that were immersed in 5% $H_2SO_4$ and 5% $Na_2SO_4$ solutions for 28 and 90 days. The names of these experiments, related standards and sample sizes are presented in Table 4.

## 3. Results and Discussion

### 3.1. Capillary water absorption

Capillary water absorption test results of concretes with different waste types and ratios are presented in Fig. 4.

**Table 4.** Experimental studies, related standards and sample sizes.

| Type of the test | Standard | Sample size |
|---|---|---|
| Capillary water absorption | ASTM C 1585 (2020) | 150x150 mm cube |
| Acid attack | ASTM C 267 (2020) | 150x150 mm cube |
| Sulfate attack | ASTM C 1012 (2019) | 150x150 mm cube |

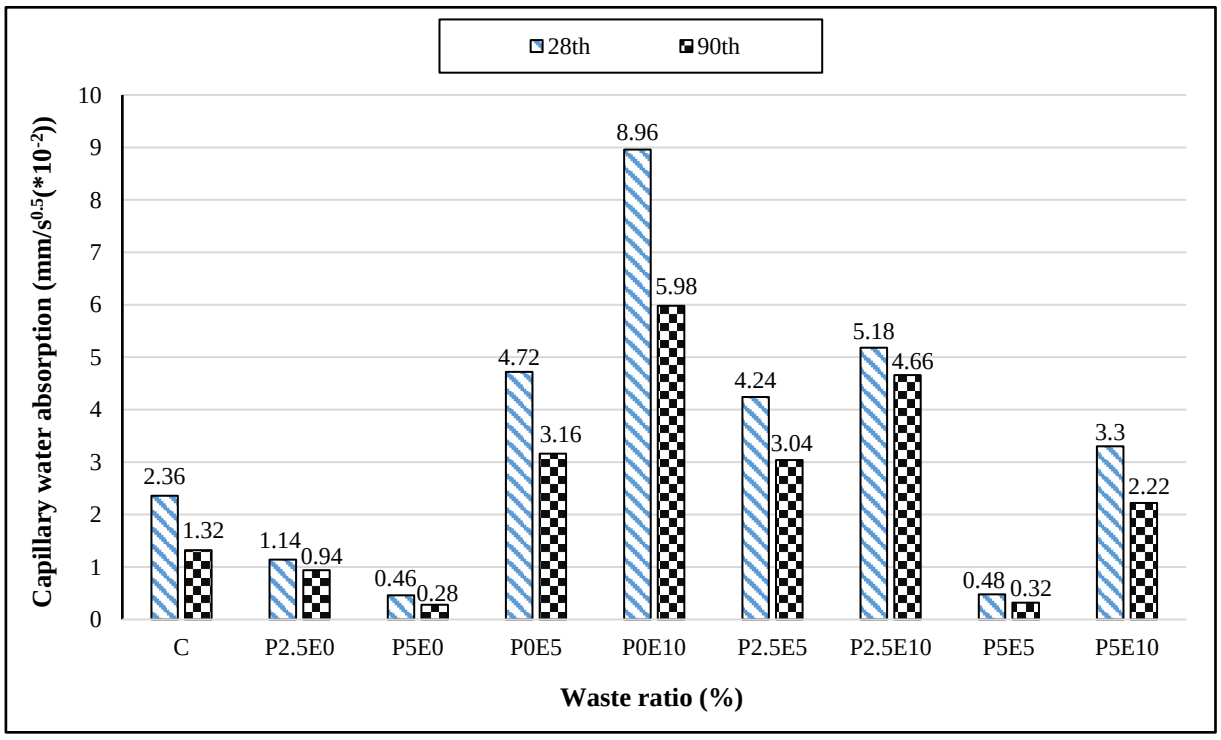


**Fig. 4.** Capillary water absorption results of concrete with different waste types and ratios.

Accordingly, the utilization of waste rubber powder in the concrete resulted in lower capillary water absorption values than the control concrete. For example, when the 28-day results are analyzed, while the capillary water absorption of the control concrete (C/28) was 2.36, this value decreased to 1.14 in concrete with 2.5% waste rubber powder (P2.5E0/28), and the capillary water absorption value decreased by 80% with a value of 0.46 in concrete produced with 5% waste rubber powder (P5E0/28). Similar situation was also ob-

served in 90 days results. Similar behavior was also reported in studies on capillary water absorption properties of waste rubber concretes (Medine et al. 2018; Steyn et al. 2021).

Capillary water absorption values increased as a result of the utilization of different ratios of e-waste in concrete. For example, when the 90-day results were analyzed, capillary water absorption of 5% e-waste concrete (P0E5/90) was 3.16, while this value was 5.98 when the e-waste ratio increased to 10% (P0E10/90). At the end of 90 days, the capillary water absorption value of 10% e-waste concrete was 4.5 times higher than the control concrete and 21 times higher than the concrete with 5% waste rubber powder. It is believed that the porous structure of e-waste is effective in obtaining this result (Ahmad et al. 2023). Parameters such as air content, presence of chemical additives, number and type of voids, aggregate properties, curing time, and hydration time are believed to be effective on capillary water absorption values of concretes (Gesoğlu and Güneyisi 2011).

When the concretes in which waste rubber powder and e-waste were combined, it was observed that the best result was obtained in concretes containing 5% waste rubber powder and 5% e-waste. The capillary water absorption values of this concrete (P5E5) were quite low with 0.48 and 0.32 for 28 and 90 days respectively. In this situation; it is considered that e-waste is hydrophobic in nature and its low water absorption capacity is effective in producing concretes with low capillary water absorption coefficient by exhibiting strong compatibility when combined with 5% waste rubber powder in the presence of 5% e-waste ratio (Manjunath 2016; Ullah et al. 2021; Ahmad et al. 2022). Additionally, as a result of the limited studies on this subject in the literature (Pedro et al. 2013; Fadiel et al. 2014; Si et al. 2017), it has been reported similar to this study that rubber aggregates used at low rates (especially 5% and less) reduce the capillarity coefficients of concrete.

It was observed that capillary water absorption values decreased in all concretes as the curing time increased. This is attributed to the increase in cement hydration over time and to the fact that the water on the wastes reduces the air voids and prevents capillary water ingress (Islam et al. 2023b).

### *3.2. Acid attack*

After 28 and 90 days of exposure to acid attack, weight loss, compressive strength loss and visual evaluations of waste rubber powder and e-waste concretes with different ratios were carried out comprehensively.

#### *3.2.1. Weight loss of acid attacked concretes*

The weight losses of the concretes after acid attack are presented in Fig. 5. The weight losses of the concretes after acid attack decreased as a result of the substitution of 2.5% and 5% waste rubber powder for cement. For example, when the 90-day results are analyzed, the weight loss of the control concrete (C/90) was 1.92%, while the weight loss of the concrete with 5% waste rubber powder (P5E0/90) was 0.42%. As observed during concrete production, other concrete components that are highly compatible with waste rubber powder exhibited superior workability, did not show any negative behavior such as crack formation or material separation in the concrete, and concretes with high resistance to acid attack could be produced (Kandil and Bulut 2023).

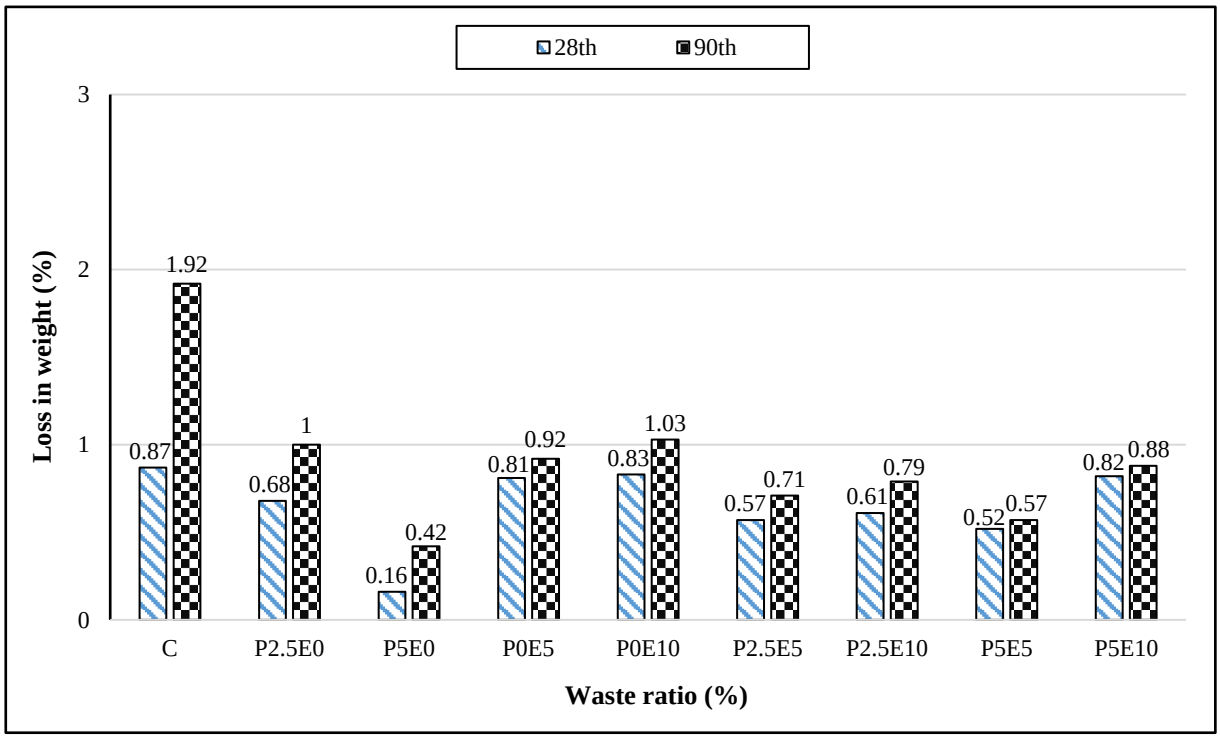


**Fig. 5.** Loss in weight results of concretes after acid attack.

When different ratios of e-waste were included in the concrete, weight losses were less than the control concrete. For example, the weight losses of concretes with 5% and 10% e-waste ratios after 28 days of acid exposure were 0.81% (P0E5/28) and 0.83% (P0E10/28), respectively. As a result of the combined utilization of both waste types in concrete, it was observed that the lowest weight loss was 0.52% and 0.57% in concretes containing 5% waste rubber powder and 5% e-waste (P5E5) after 28 and 90 days, respectively.

After 28 and 90 days of exposure to acid, the weight losses of concretes containing waste rubber powder and e-waste were lower than the control concrete. This indicates that more resistant concretes can be produced against acid attack by incorporating two waste types in concrete.

### *3.2.2. Compressive strength loss of acid attacked concretes*

The compressive strengths of the concretes before and after acid and sulfate exposure were carried out according to TS EN 12390-3 (2019) standard and given in Table 5. Based on the results in Table 5, In Fig. 6, the compressive strength losses of concretes with different types and ratios after 28 and 90 days of exposure to acid attack are provided in percentages.

**Table 5.** Initial compressive strength results of concretes before acid and sulfate tests.

| Code | 28-day compressive strength (MPa) | 90-day compressive strength (MPa) |
|---|---|---|
| C | 41.10 | 44.50 |
| P2.5E0 | 48.60 | 51.40 |
| P5E0 | 44.00 | 48.40 |
| P0E5 | 39.00 | 42.90 |
| P0E10 | 19.20 | 23.40 |
| P2.5E5 | 42.00 | 44.80 |
| P2.5E10 | 24.50 | 28.80 |
| P5E5 | 35.20 | 36.20 |
| P5E10 | 29.30 | 32.00 |

According to Fig. 6, it is observed that the utilization of waste rubber powder has a decreasing effect on the compressive strength loss of concretes after acid attack compared to the control concrete, while e-waste has an increasing effect. For example, when the 28-day results are analyzed, while the compressive strength loss of the control concrete (C/28) was 16.06%, this loss decreased by 23% to 12.39% in concrete with 5% waste rubber powder (P5E0/28), and increased by 30% to 22.8% with 10% e-waste. The lowest compressive strength loss was observed for all days in concretes containing 5% waste rubber powder and 5% e-waste (P5E5).

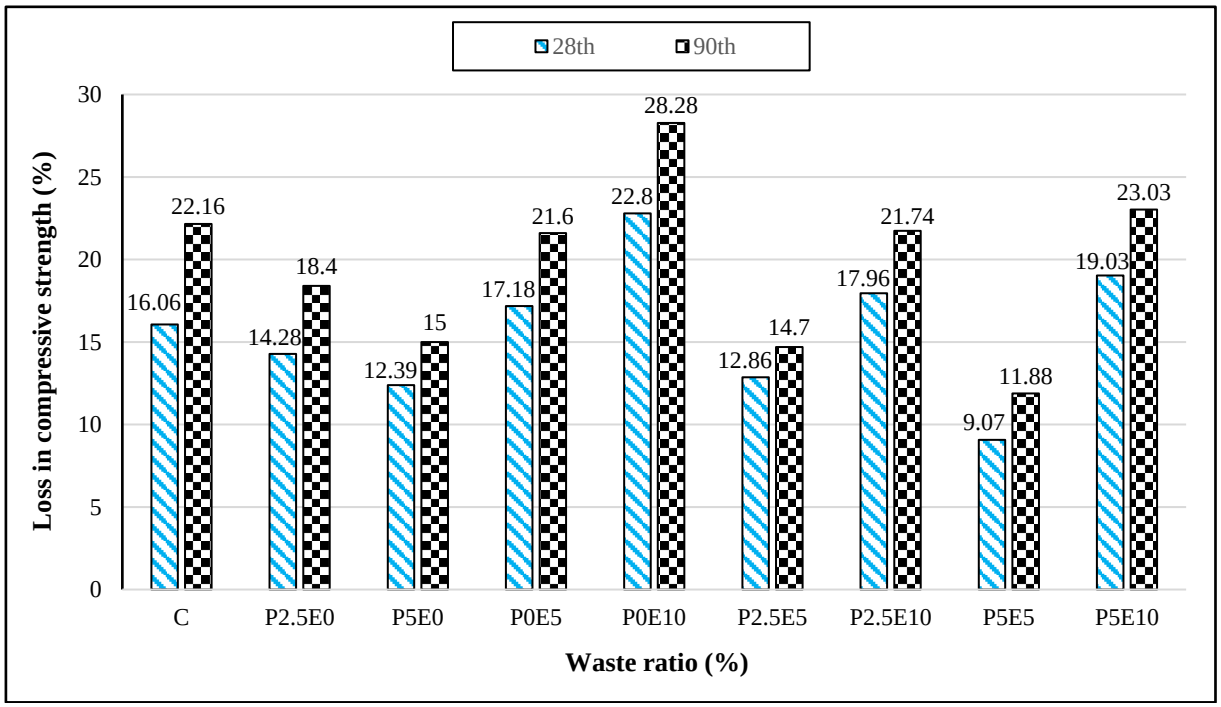


**Fig. 6.** Loss in compressive strength results of concretes after acid attack.

In general, compressive strength losses increased in all concrete groups after acid exposure from 28 days to 90 days. It is thought that the strength losses experienced by concretes after acid exposure may be due to the negative impact of the cement paste, especially as a result of long-term acid exposure, deterioration of the e-waste (aggregate)-matrix interface, and decreases in strength with the increase of microcracks (Kajorncheappunngam et al. 2002; Ghassemi and Toufigh 2020). As a result of the study, it can be stated that especially waste rubber powder can make concretes more resistant to acid attack. Considering that concretes containing 2.5% waste rubber powder-5% e-waste and 5% waste rubber powder-5% e-waste experienced less weight and compressive strength loss than the control concrete, it can be stated that they can be evaluated together in concretes that will be exposed to acid.

*3.2.3. Visual evaluation results of acid attacked concretes*

Fig. 7 presents the visual results of the concretes subjected to acid attack for 90 days. Accordingly, the visual damages of the specimens displayed a similar trend to the weight and compressive strength losses. It is clearly observed in a and b images that concrete with 5% waste rubber powder (P5E0/90) and concrete with 5% waste rubber powder-5% e-waste (P5E5/90), which are the concretes with the lowest weight and compressive strength losses, are visually more resistant to acid exposure. Control concrete (C/90) and concrete containing 10% e-waste (P0E10/90) suffered more visual damage (surface peeling, discolouration, abrasion, exfoliation) as a result of acid attack (visible in images c and d). This coincided with the weight and compressive strength losses.


**Fig. 7.** Images of concretes exposed to acid attack for 90 days:
(a) 5% waste rubber powder added concrete (P5E0/90);
(b) 5% waste rubber powder and 5% e-waste added concrete (P5E5/90);
(c) Control concrete (C/90); (d) 10% e-waste added concrete (P0E10/90).

### *3.3. Sulfate attack*

Weight loss, compressive strength loss and visual evaluations of concretes containing waste rubber powder and e-waste subjected to sulfate attack on different days were analyzed in detail.

#### *3.3.1. Weight loss of sulfate attacked concretes*

Fig. 8 presents the weight losses of the concretes exposed to sulfate attack for 28 and 90 days.

The results obtained are remarkable and engaging for the literature and all of the concrete groups experienced weight increases instead of weight losses. For example, when the 90-day results were analyzed, the highest weight loss/increase was observed in concrete containing 5% waste rubber powder-10% e-waste (P5E10/90) and concrete containing 5% waste rubber powder-5% e-waste (P5E5/90) with values of -1% and -0.74%, respectively. When the sulfate attack increased from 28 days to 90 days, the weight increases in the concretes also increased. Sulfate attack is a complex mechanism with mechanical, chemical and physical processes and negatively affects the properties of concrete (Tanyildizi 2016; Ikumi et al. 2019). It is believed that sulfate ions blocked the pores of the concretes and caused an increase in weight. In addition, it is considered that the high absorption ability and deformation capacity of both waste types in the face of energy increase, which will reduce the entry and reactivity of sulfate ions into the internal structure, are effective in this situation (Onuaguluchi and Banthia 2019). It was determined that the weight losses/increases after the sulfate attack were similar to each other and very close to 0. This showed that concretes produced with waste rubber powder and e-waste can be resistant to sulfate attack.

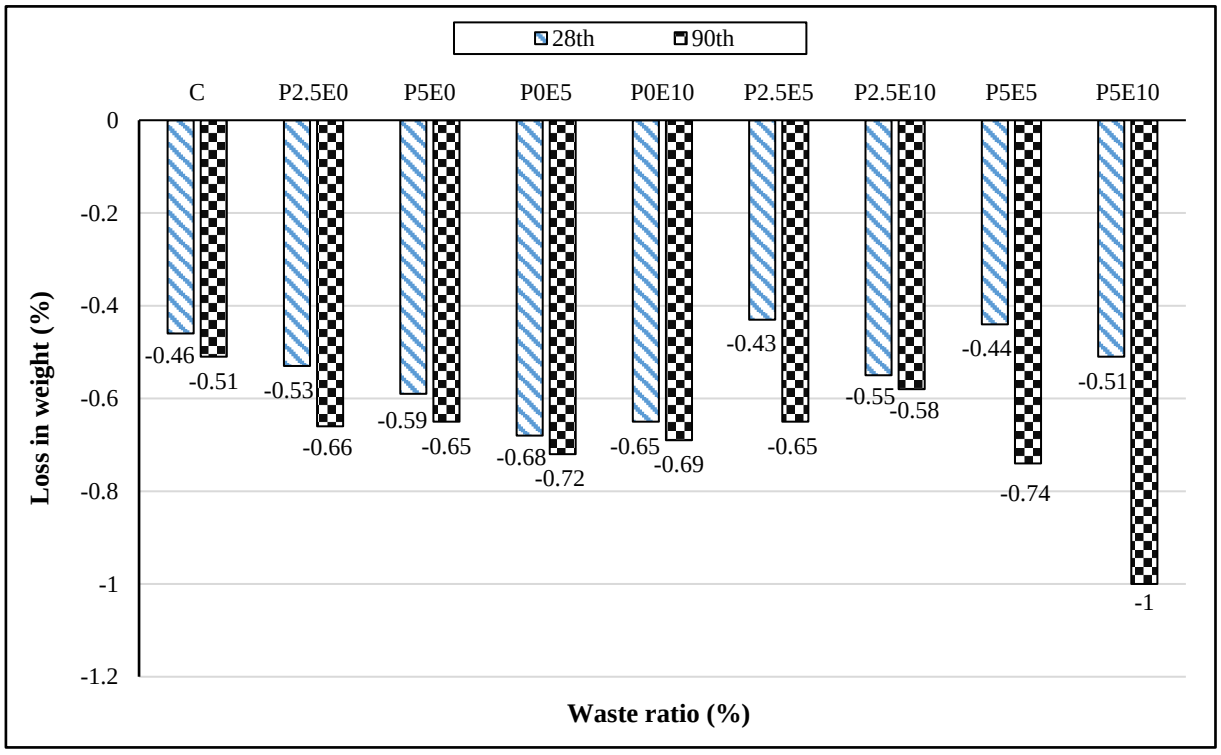


**Fig. 8.** Loss in weight results of concretes after sulfate attack.

#### *3.3.2. Compressive strength loss of sulfate attacked concretes*

Based on the results in Table 5, Fig. 9 illustrates the compressive strength losses due to sulfate attack depending on the day parameter on concretes with different proportions of waste rubber powder and e-waste.

From Fig. 9, it is clearly observed that the utilization of increasing proportions of waste rubber powder in concrete results in lower compressive strength loss after sulfate attack compared to the control concrete. For example, while the compressive strength loss experienced by the control concrete (C/28) after 28 days of sulfate attack was 6.81%, this loss decreased approximately 7 times less to 0.91% in concrete with 5% waste rubber powder (P5E0/28). The use of e-waste resulted in higher compressive strength losses. For example, after 90 days of sulfate attack, the compressive strength loss of 5% e-waste concrete (P0E5/90) was 13.84%, while the compressive strength loss of 10% e-waste concrete (P0E10/90) increased approximately 2 times to 25.39%. These two concretes had the highest compressive strength loss among all groups at the end of 90 days. It is considered that the strength losses of e-waste concretes after sulfate attack are affected by the fact that sulfate ions move more easily at the aggregate-matrix interface, which weakens and voids increase with the increase in ratio, negatively affecting the adherence and causing an increase in cracks (Griffiths and Ball 2000; Hashemi et al. 2018).

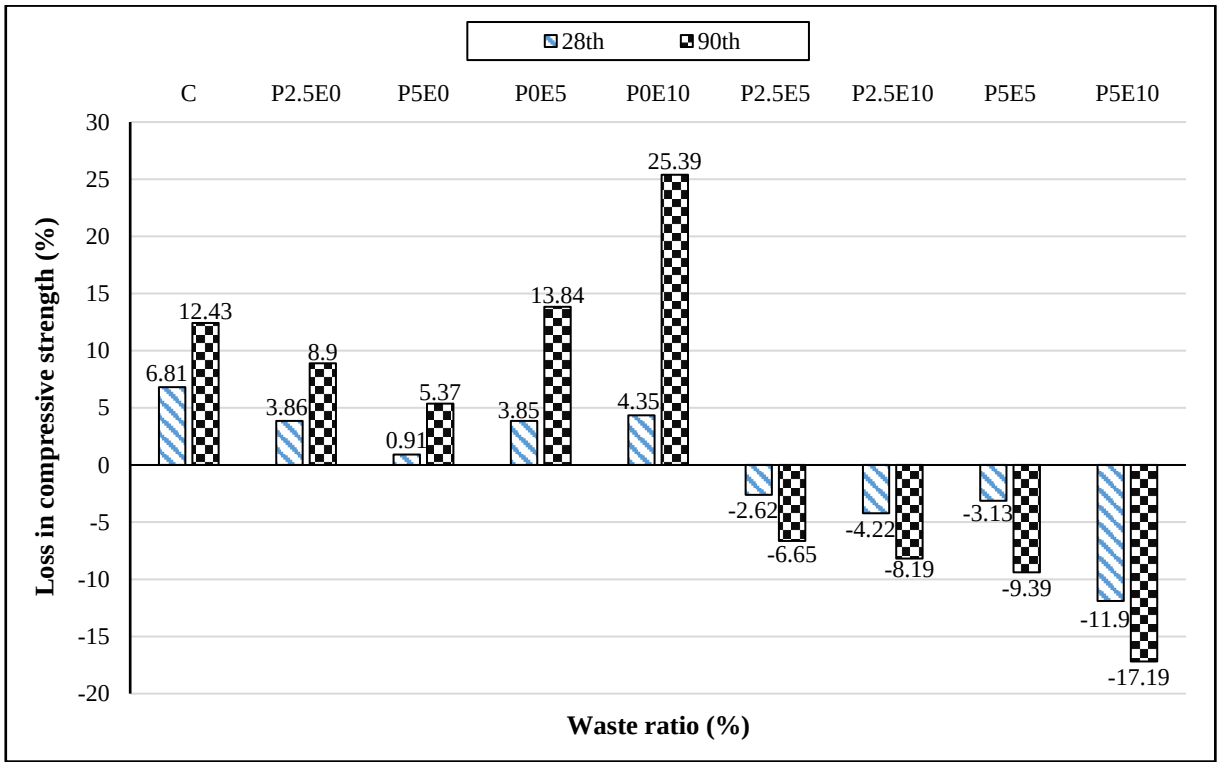


**Fig. 9.** Loss in compressive strength results of concretes after sulfate attack.

As a result of the combination of waste rubber powder and e-waste in concrete, interesting results were obtained for compressive strength losses after sulfate exposure. For example, at the end of 90 days, concrete containing 5% waste rubber powder and 5% e-waste (P5E5/90) and concrete containing 5% waste rubber powder and 10% e-waste (P5E10/90) did not lose compressive strength after sulfate attack, but on the contrary, their compressive strengths increased. These values were obtained as -9.39% and -17.19%, respectively. A similar pattern was observed in the concretes in which two waste types with lower ratios were combined. It was determined that the compressive strength losses of the concretes in which waste rubber powder and e-waste were utilized together against sulfate attack were positively differentiated from both control concrete and concretes produced using single waste type. For this study, it was determined that, with the ideality of the waste ratios, these expandable products can be applied to the walls of concrete voids, such as gypsum, ettringite and tomasite, which may occur due to sulfate attack in the internal structure of concretes produced by using both e-waste and waste rubber powder together at low rates. It is thought that the crystallization pressure is less and does not have a negative effect on the strength. (Scherer 2004).

### *3.3.3. Visual evaluation results of sulfate attacked concretes*

Fig. 10 presents the visual results of concretes exposed to sulfate attack for 90 days. It was observed that 5% waste rubber powder-10% e-waste concrete (P5E10/90) and 5% waste rubber powder-5% e-waste concrete (P5E5/90), which differed from other concretes in a positive way in terms of both weight and compressive strength loss, did not suffer any significant damage after sulfate attack, as can be observed in a and b images. However, concrete with 5% e-waste (P0E5/90) and concrete with 10% e-waste (P0E10/90) were severely damaged after sulfate attack (chipping, peeling, cracking, discolouration at the corners) as can be clearly visualised in images c and d. The results of the visual analysis were similar to the weight and compressive strength losses obtained after sulfate attack.

## 4. Conclusions

The results obtained from this study, in which capillary water absorption, acid and sulfate attack experiments of concrete were carried out depending on the day parameter as a result of the utilization of e-wastes and waste rubber powder in concrete at different ratios, are summarized below:

- Capillary water absorption values of the concretes in which waste rubber powder was utilized instead of cement were lower than the control concrete. Capillary water absorption values of concretes produced using e-waste increased. At the end of 90 days, capillary water absorption value of 10% e-waste concrete was 4.5 times higher than control concrete and 21 times higher than 5% waste rubber powder concrete.
- The weight losses of concretes containing waste rubber powder and e-waste exposed to acid for 28 and 90 days were lower than the control concrete. It was determined that the utilisation of waste rubber pow-

der had a decreasing effect on the compressive strength losses of concretes after acid attack compared to control concrete, while e-waste had an increasing effect.

- All of the concrete groups exposed to sulfate attack experienced weight increases instead of weight losses. These increases were similar to each other and very close to 0. It was observed that the utilisation of increasing amounts of waste rubber powder in concrete resulted in lower compressive strength loss after sulfate attack compared to the control concrete. The use of e-waste resulted in higher compressive strength losses.
- In parallel with the weight and compressive strength losses obtained after acid and sulfate attack, the visual analysis results of the concretes were similar.
- When the test results are evaluated in general, the use of 5% waste rubber powder in concrete individually brought the best results. In addition, among the concretes in which e-waste and waste rubber powder were utilized together, the ideal ratios were determined as 5% waste rubber powder 5% e-waste.
- In terms of both the protection of natural resources and sustainability, it is significant for the literature to determine that waste rubber powder can be utilized instead of cement and e-waste can be substituted for aggregate in concrete production as a result of this study.


**Fig. 10.** Images of concretes exposed to sulfate attack for 90 days:
(a) 5% waste rubber powder and 10% e-waste added concrete (P5E10/90);
(b) 5% waste rubber powder and 5% e-waste added concrete (P5E5/90);
(c) 5% e-waste added concrete (P0E5/90); (d) 10% e-waste added concrete (P0E10/90).

***Acknowledgements***

*None declared.*

***Funding***

*The author received no financial support for the research, authorship, and/or publication of this manuscript.*

***Conflict of Interest***

*The author declared no potential conflicts of interest with respect to the research, authorship, and/or publication of this manuscript.*

***Data Availability***

*The datasets created and/or analyzed during the current study are not publicly available, but are available from the corresponding author upon reasonable request.*

## REFERENCES

AbdelAleem BH, Hassan AAA (2022). Use of rubberized engineered cementitious composite in strengthening flexural concrete beams. *Engineering Structures*, 262, 114304.

Ahmad F, Qureshi MI, Ahmad Z (2022). Influence of nano graphite platelets on the behavior of concrete with E-waste plastic coarse aggregates. *Construction and Building Materials*, 316, 125980.

Ahmad Z, Alsulamy S, Raza A, Salmi A, Abid M, Deifalla AF, Khadimallah MA, Elhadi KM (2023). Life cycle assessment (LCA) of polypropylene fibers (PPF) on mechanical, durability, and microstructural efficiency of concrete incorporating electronic waste aggregates. *Case Studies in Construction Materials*, 18, e01979.

Alagusankareswari K, Kumar SS, Vignesh KB, Niyas AH (2016). An experimental study on e-waste concrete. *Indian Journal of Science and Technology*, 9(2), 1-5.

ASTM C 1585 (2020). Standard test method for measurement of rate of absorption of water by hydraulic-cement concretes. ASTM International, West Conshohocken, PA, USA.

ASTM C 267 (2020). Standard test methods for chemical resistance of mortars, grouts, and monolithic surfacings and polymer concretes. ASTM International, West Conshohocken, PA, USA.

ASTM C 1012 (2019). Standard test method for length change of hydraulic-cement mortars exposed to a sulfate solution. ASTM International, West Conshohocken, PA, USA.

Bahtli T, Ozbay N (2021). Mechanical properties and freeze-thaw resistances of bronze-concrete composites. *Challenge Journal of Concrete Research Letters*, 12(2), 39-48.

Bhutta MKS, Omar A, Yang X (2011). Electronic waste: A growing concern in today's environment. *Economics Research International*, 1-8.

Bulut HA, Şahin R (2017). A study on mechanical properties of polymer concrete containing electronic plastic waste. *Composite Structures*, 178, 50-62.

Bulut HA (2024). Evaluation of the impact of waste on the mechanical performance of concrete. *5th International Azerbaijan Congresses on Life, Engineering, Mathematical, and Applied Sciences*, Baku, Azerbaijan, 87-93.

Canbaz M, Kara İ, Topçu İ (2021). Effect of high temperature on the mechanical behavior of cement-bonded wood composite produced with wood waste. *Challenge Journal of Structural Mechanics*, 7(1), 42-48.

Colette DA, Martial AKD, Joseph AY, Benjamin YK, Patrick DA (2023). Optimization of the compressive strength of used tire/cement phase composite concretes using a full factorial design. *Construction and Building Materials*, 404, 133252.

Fadiel A, Al Rifaie F, Abu-Lebdeh T (2014). Use of crumb rubber to improve thermal efficiency of cement-based materials. *American Journal of Engineering and Applied Sciences*, 7(1), 1-11.

Farooq A, Abid MM, Tariq T, Riaz M, Haroon W, Malik AA, Rehman U (2019). Impact on concrete properties using e-plastic waste fine aggregates and silica fume. *Gospodarka Surowcami Mineralnymi - Mineral Resources Management*, 35(2), 103-118.

Ferreira L, Brito JD, Saikia N (2012). Influence of curing conditions on the mechanical performance of concrete containing recycled plastic aggregate. *Construction and Building Materials*, 36, 196-204.

Gao X, Yang J, Shao J, Zhu H, Xu J, Haruna SI (2024). Regulation of carbon nanotubes on internal humidity of concrete with recycled tire rubber: Mechanism analysis and modeling. *Journal of Building Engineering*, 82, 108253.

Gawatre D, Damal V, Londhe S, Mane A, Ghawate H (2015). Environmental issues of plastic waste use in concrete. *International Journal of Innovative Research in Advanced Engineering*, 2(5), 114-118.

Gesoglu M, Güneyisi E, Hansu O, Etli S, Alhassan M (2017). Mechanical and fracture characteristics of self-compacting concretes containing different percentage of plastic waste powder. *Construction and Building Materials*, 140, 562-569.

Gesoğlu M, Güneyisi E (2011). Permeability properties of self-compacting rubberized concretes. *Construction and Building Materials*, 25(8), 3319-3326.

Ghassemi P, Toufigh V (2020). Durability of epoxy polymer and ordinary cement concrete in aggressive environments. *Construction and Building Materials*, 234, 117887.

Griffiths R, Ball A (2000). An assessment of the properties and degradation behaviour of glass-fibre-reinforced polyester polymer concrete. *Composites Science and Technology*, 60(14), 2747-2753.

Hameed HB, Ali Y, Petrillo A (2020). Environmental risk assessment of E-waste in developing countries by using the modified-SIRA method. *Science of the Total Environment*, 733, 138525.

Hashemi MJ, Jamshidi M, Aghdam JH (2018). Investigating fracture mechanics and flexural properties of unsaturated polyester polymer concrete (UP-PC). *Construction and Building Materials*, 163,767-775.

Helmy SH, Tahwia AM, Mahdy MG, Elrahman MA (2023). Development and characterization of sustainable concrete incorporating a high volume of industrial waste materials. *Construction and Building Materials*, 365, 130160.

Ikumi T, Cavalaro SH, Segura I (2019). The role of porosity in external sulphate attack. *Cement and Concrete Composites*, 97, 1-12.

Islam MMU, Li J, Roychand R, Saberian M (2023a). Microstructure, thermal conductivity and carbonation resistance properties of sustainable structural lightweight concrete incorporating 100% coarser rubber particles. *Construction and Building Materials*, 408, 133658.

Islam MMU, Li J, Roychand R, Saberian M (2023b). Investigation of durability properties for structural lightweight concrete with discarded vehicle tire rubbers: A study for the complete replacement of conventional coarse aggregates. *Construction and Building Materials*, 369, 130634.

Kajorncheappunngam S, Gupta RK, GangaRao HVS (2002). Effect of aging environment on degradation of glass-reinforced epoxy. *Journal of Composites for Construction*, 6(1).

Kandil U, Bulut HA (2023). Examination of the permeability of rubberized concrete with different water/cement ratios and their resistance against acid and sulfate attack. *Progress in Rubber, Plastics and Recycling Technology*, Article In Press.

Karalar M, Çavuşlu M (2022). Evaluating effects of granulated glass on structural and seismic behavior of tall RC structures using experimental tests and 3D modeling. *Challenge Journal of Structural Mechanics*, 8(2), 63-77.

Jiang Z, Easa SM, Hu C, Zheng X (2019). Understanding damping performance and mechanism of crumb rubber and styrene-butadiene-styrene compound modified asphalts. *Construction and Building Materials*, 206, 151-159.

Jurado J, Zubiarrain NM, Villa EI, Rocco CG, Braun M (2023). Mesoscale modelling of the mechanical behaviour of concrete with rubber as coarse aggregate. *Engineering Fracture Mechanics*, 291, 109533.

Kiddee P, Naidu R, Wong MH (2013). Electronic waste management approaches: An overview. *Waste Management*, 33(5), 1237-1250.

Ma Q, Mao Z, Zhang J, Du G, Li Y (2023). Behavior evaluation of concrete made with waste rubber and waste glass after elevated temperatures. *Journal of Building Engineering*, 78, 107639.

Manjunath BTA (2016). Partial replacement of e-plastic waste as coarse-aggregate in concrete. *Procedia Environmental Sciences*, 35, 731-739.

Medine M, Trouzine H, Aguiar JBD, Asroun A (2018). Durability properties of five years aged lightweight concretes containing rubber aggregates. *Periodica Polytechnica Civil Engineering*, 62(2), 386-397.

Moustafa A, ElGawady MA (2015). Mechanical properties of high strength concrete with scrap tire rubber. *Construction and Building Materials*, 93, 249-256.

Onuaguluchi O, Banthia N (2019). Long-term sulfate resistance of cementitious composites containing fine crumb rubber. *Cement and Concrete Composites*, 104, 103354.

Partheeban P, Kalaiyarrasi ARR, PB LN (2021). Performance evaluation of geopolymer concrete using E-waste and M-sand. *Research on Engineering Structures and Materials*, 7(2), 183-198.

Pedro D, De Brito J, Veiga R (2013). Mortars made with fine granulate from shredded tires. *Journal of Materials in Civil Engineering*, 25(4), 519-529.

Qaidi SMA, Dinkha YZ, Haido JH, Ali MH, Tayeh BA (2021). Engineering properties of sustainable green concrete incorporating eco-friendly aggregate of crumb rubber: A review. *Journal of Cleaner Production*, 324, 129251.

Scherer GW (2004). Stress from crystallization of salt. *Cement and Concrete Research*, 34(9), 1613-1624.

Si R, Guo S, Dai Q (2017). Durability performance of rubberized mortar and concrete with NaOH-solution treated rubber particles. *Construction and Building Materials*, 153, 496-505.

Steyn ZC, Babafemi AJ, Fataar H, Combrinck R (2021). Concrete containing waste recycled glass, plastic and rubber as sand replacement. *Construction and Building Materials*, 269, 121242.

Suchithra S, Manoj K, Indu VS (2015). Study on replacement of coarse aggregate by e-waste in concrete. *International Journal of Technical Research and Applications*, 3(4), 266-270.

Şengel H, Kınık K, Erol H, Canbaz M (2022a). Effect of waste steel tire wired concrete on the mechanical behavior under impact loading. Challenge Journal of Structural Mechanics, 8(4), 150-158.

Şengel H, Özgören A, Erol H, Canbaz M (202b). Mechanical behavior investigation of rubberized concrete barriers in impact load. Challenge Journal of Concrete Research Letters, 13(3), 93-100.

Tanyildizi H (2016). The investigation of microstructure and strength properties of lightweight mortar containing mineral admixtures exposed to sulfate attack. *Measurement*, 77, 143-154.

Thomas BS, Gupta RC, Panicker VJ (2016). Recycling of waste tire rubber as aggregate in concrete: durability-related performance. Journal of Cleaner Production, 112 (Part 1), 504-513.

TS EN 933-1 (2012). Tests for geometrical properties of aggregates part 1: Determination of particle size distribution sieving method. Turkish Standards Institution, Ankara, Turkey, (Turkish Codes).

TS 802 (2016). Design of concrete mixes. Turkish Standards Institution, Ankara, Turkey, (Turkish Codes).

TS EN 12390-3 (2019). Testing hardened concrete part 3: Compressive strength of test specimens. Turkish Standards Institution, Ankara, Turkey, (Turkish Codes).

Ullah Z, Qureshi MI, Ahmad A, Khan SU, Javaid MF (2021). An experimental study on the mechanical and durability properties assessment of E-waste concrete. *Journal of Building Engineering*, 38, 102177.

Ullah K, Qureshi MI, Ahmad A, Ullah Z (2022). Substitution potential of plastic fine aggregate in concrete for sustainable production. *Structures*, 35, 622-637.

Xu J, Niu X, Ma Q, Han Q (2021). Mechanical properties and damage analysis of rubber cement mortar mixed with ceramic waste aggregate based on acoustic emission monitoring technology. *Construction and Building Materials*, 309, 125084.

Youssf O, Mills JE, Benn T, Zhuge Y, Ma X, Roychand R, Gravina R (2020). Development of crumb rubber concrete for practical application in the residential construction sector – design and processing. *Construction and Building Materials*, 260, 119813.

Challenge Journal of Concrete Research Letters

Research Article

# Enhancing mechanical properties of foam concrete with sisal fiber reinforcement: An experimental investigation

Mehmet Uzun [a,*]

[a] *Department of Civil Engineering, Karamanoğlu Mehmetbey University, 70200 Karaman, Türkiye*

**ABSTRACT**

In this study, we explore the possibility of using sisal fibers as an environmentally-friendly reinforcing agent for foam concrete. We aim to improve its physical properties by combining environmental friendliness with engineering practicality to create a durable material that can be used safely today and a supplier of ecological sustainability for tomorrow. Known for being lightweight and thermally insulating, foam concrete has very low tensile strength and ductility as compared with other materials. This is why its application is often limited in scope. We naturally think that adding sisal fibers, which are a high-performance and renewable resource in themselves, will improve these properties. It is well known that they have a tensile strength of more than 400 kg/cm, and their long, stiff lamellae further increase this advantage. As a result, we integrated sisal fibers at different mixing rates: 0 (no Sisal), 0.25g, 0.5g and so on up to 1% volume. After the test specimens were standardized like this they went into the hence examining each of these properties in turn. With a reasonable content of fibres, the mechanical properties of foam concrete improved significantly. It was observed that the properties of fresh concrete decreased slightly in the samples where 0.50% sisal fiber was used. However, the compressive strength increased by 12.9% compared to the reference sample, and the flexural strength increased by 2.85 times compared to the reference sample. This study not only confirms the feasibility of using sisal fibers to reinforce foam concrete theoretically, but it will also serve as a useful reference for the development of more sustainable scientific building materials. The author provides a discussion of their results and future directions for research on construction materials, highlighting environmental and economic benefits from incorporating natural fibers into these materials.

**ARTICLE INFO**

*Article history:*
Received 22 March 2024
Revised 18 April 2024
Accepted 29 April 2024

*Keywords:*
Natural fibers
Sisal fibers
Foam concrete
Mechanical properties



## 1. Introduction

Foam concrete is an ideal construction material, characterized by its cellular structure made of a mixture of cement, sand, water, and foaming agent, that combines the best of lightweight form, thermal insulation, and sound absorption (Raj et al. 2019; Shi et al. 2021; Tran et al. 2022; Shaheen et al. 2023). Traditionally, it has been applied in construction for non-load-bearing walls, insulation panels, and void filling, as a result of the relatively low density and good thermal performance it brings (Hamada et al. 2023). However, despite these advantages, foam concrete has its weaknesses in mechanical strength and durability that confine its use to parts of a building structure that are not bearing considerable load (Falliano et al. 2018).

Foam concrete's intrinsic properties, such as low density and high thermal insulation, make it an attractive choice for specific construction applications. However, its broader use is hampered by limited mechanical strength and durability. Studies exploring ways to enhance these properties have focused on various admixtures and reinforcements (Huang et al. 2015; Ji et al. 2015; Oren et al. 2020). For instance, Jones and McCarthy (2005) demon-

* *Corresponding author*. Tel.: +90-338-226-2200 E-mail address: mehmetuzun@kmu.edu.tr (M. Uzun)
ISSN: 2548-0928 / DOI: https://doi.org/10.20528/cjcrl.2024.03.002

strated that the inclusion of synthetic fibers could marginally improve the compressive strength of foam concrete. Similarly, a study by Renjith et al. (2021) explored the use of micro-silica to enhance the material's mechanical properties, noting improvements in both compressive and flexural strengths. Despite these advancements, the environmental impact of synthetic reinforcements remains a concern. This has led researchers to explore natural, sustainable alternatives that would not compromise the material's performance (Jones and McCarthy 2005). The exploration of natural fibers as reinforcement in construction materials has surged due to their environmental benefits over synthetic fibers. Natural fibers, including bamboo, hemp, flax, and sisal, have been investigated for their potential to enhance the mechanical properties of construction materials (Coutts and Ni 1995; Frydrych et al. 2019; Netinger Grubeša et al. 2018; Okeola et al. 2018). In addition to their ability to deliver high structural performance, low density, high acoustic damping and reduced industrial fuel expense, the use of natural fiber-reinforced composite materials has been proposed to provide optimal recyclability and biodegradability (Çakıroğlu and Bekdaş 2021; Gultekin 2023). Wang et al. (2023) provided an extensive review of the mechanical properties of natural fiber-reinforced concrete, emphasizing the positive impact of natural fibers on improving tensile strength, flexural strength, and crack resistance. Due to the high mechanical properties of natural fibers, natural fiber added concretes are preferred not only in structural elements but also in non-structural elements. Due to its high tensile strength, it is very common to use it as a wall element, as a superstructure element for roads, and in underground systems. Sisal fiber stands out due to its availability, cost-effectiveness, and mechanical properties. Its application in construction materials has been limited but promising, with studies showing its potential to improve not only the mechanical properties but also the thermal and acoustical insulation of composites (Shalwan et al. 2017).

The construction industry, today a major cause of global carbon emissions, is under increasing pressure to shift towards more sustainable practices. Part of this shift involves seeking out green building materials which not only meet structural requirements but also reduce the environmental effects of their production and use. In this context, natural fibers used for reinforcement in construction materials make sense. Renewable, biodegradable and having a low carbon footprint, natural fibers are well partnered with the aims of sustainable construction (Zini and Scandola 2011).

One method to enhance the mechanical properties of concrete is by adding fibers to the concrete mix (Canbaz et al. 2022). Of the natural fibers available, sisal, in particular, has attracted attention because it has high tensile strength, durability and resistance to degradation in harsh environments (Ahmad et al. 2022). In this way, it is suitable for use in buildings where it may be exposed to chemicals and some similar harsh conditions. Sisal fiber derived from the Agave sisalana plant is traditionally employed in the manufacture of rope or twine but has been more recently proposed as reinforcement for polymer composites and building materials (Sabarish et al. 2020).

Sisal fiber's potential in reinforcing construction materials, particularly in foam concrete, has garnered attention in recent years. A pivotal study by Zhang et al. (2024) investigated the effects of sisal fiber on the compressive and tensile strengths of foam concrete. They found that small additions of sisal fibers could significantly enhance the material's ductility while marginally improving its compressive strength. This study laid the groundwork for further exploration into the optimal percentage of sisal fiber inclusion for maximizing mechanical benefits.

Moreover, a recent research has begun to address the long-term durability of sisal fiber-reinforced foam concrete under various environmental conditions. Naik et al. (2024) explored the effects of moisture and microwaves on the mechanical properties of sisal fiber-reinforced composites, highlighting the fibers' resilience and the composite's maintained integrity over time.

The utilization of natural fiber, such as sisal, is an environmentally friendly way to improve the mechanical properties of composite materials due to its excellent properties. However, specific records of how this fine product should for the best parameters used in foam concrete construction do not exist. Addressing this gap has both theoretical and practical worth, benefiting the environment too. This paper fills this area, promoting in greater depth a better understanding of renewable materials in construction-able objects, and thereby furthering on sustainable development of our construction. In this study, sisal fiber-added foam concrete samples were prepared. Fiber ratios of 0.25, 0.50, 0.75 and 1.00% by volume were used in the samples. The effect of the amount of fiber changing on the fresh and hardened concrete properties of foam concrete was examined.

## 2. Experimental Program

River sand with a specific gravity of 1.68 g/cm$^3$ was used as fine aggregate for the concrete mixture. Fine aggregate gradation is presented in Fig. 1.

Mixtures were prepared with CEM I 42.5R type cement, whose specific gravity and specific surface area are 3.02 g/cm$^3$ and 3150 cm$^2$/g, respectively (TS-EN-197-1 2000). The physical and chemical properties of cement are given in Table 1.

Foaming agents and foam stabilizers were used to produce foam concrete. The foaming agent is a material that facilitates foam formation. Foam stabilizer makes the foams in fresh concrete long-lasting. In this way, the porous structure in foam concrete is preserved during the concrete setting. A foam stabilizer based on Calcium stearate was used for the production of foam concrete. A protein-based foaming agent was also used for foam production. The production of foam concrete is presented in Fig. 2.

Sisal fiber was used to increase the mechanical properties of foam concrete. Sisal fiber is a type of natural fiber obtained from the Agave sisalana plant. Agave sisalana plant is a plant native to Kenya, Tanzania and Brazil. Sisal leaves are dark green and have straight flesh. Sisal leaves are crushed with a smooth-edged stick until they are separated into fibers. The fibers are then

cleaned with plenty of water to get rid of dust and waste. The cleaned fibers are air-dried. Sisal fiber is presented in Fig. 3. The physical and chemical properties of sisal fiber are given in Table 2.

**Table 1.** Physical and chemical properties of cement.

| Chemical properties (%) | | Physical and mechanical properties | |
|---|---|---|---|
| $SO_3$ | 4.12 | Initial setting time (min.) | 165 |
| CaO | 69.51 | Final setting time (min.) | 210 |
| $SiO_2$ | 13.45 | 2-days compressive strength (MPa) | 34.3 |
| MgO | 1.03 | 28-days compressive strength (MPa) | 51.8 |
| $Fe_2O_3$ | 7.34 | Specific gravity (g/cm³) | 3.02 |
| $Na_2O$ | 0.59 | Specific surface (cm²/g) | 3150 |
| $Al_2O_3$ | 3.94 | | |

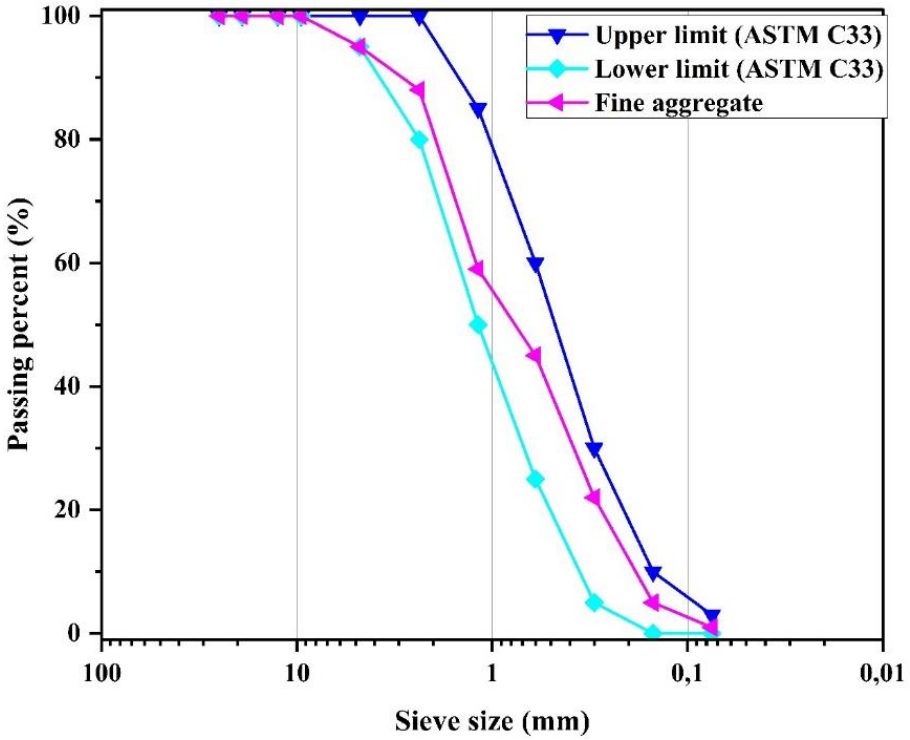


**Fig. 1.** Aggregate gradation.

**Table 2.** Physical and chemical properties of sisal fiber.

| Chemical properties (%) | | Physical and mechanical properties | |
|---|---|---|---|
| Hemicellulose | 12.3-14.6 | Density (g/cm³) | 1.36-1.41 |
| Cellulose | 66.0-74.0 | Diameter (mm) | 0.10-0.13 |
| Pectin | 10.0 | Tensile strength (MPa) | 540-720 |
| Wax | 2.0 | Elasticity modulus (GPa) | 9.0-12.4 |
| Lignin | 7.4-10.3 | | |

**Fig. 2.** Foamed concrete production.

**Fig. 3.** Agave sisalana plant and sisal fiber.

The samples using different proportions of sisal fiber were prepared to examine the effect of sisal fiber on the fresh and mechanical properties of concrete. Fresh and hardened concrete properties were examined for samples to which sisal fiber was added at 0.25, 0.50, 0.75 and 1.00% by volume. The mixtures are given in Table 3.

**Table 3.** Mix design.

| Mix | Sisal fiber % (by volume) | Cement (kg) | W/C | Fine aggregate (kg) | Foaming agent and stabilizer (kg) |
|---|---|---|---|---|---|
| R | 0 | 720 | 0.48 | 230 | 2.2/1.4 |
| SF0.25 | 0.25 | 720 | 0.48 | 230 | 2.2/1.4 |
| SF0.50 | 0.50 | 720 | 0.48 | 230 | 2.2/1.4 |
| SF0.75 | 0.75 | 720 | 0.48 | 230 | 2.2/1.4 |
| SF1.00 | 1.00 | 720 | 0.48 | 230 | 2.2/1.4 |

The mini-slump test was performed to measure the spreading diameter of fresh concrete, according to TS-EN 1170-1 (TS-EN-1170-1 1999), as shown in Fig. 4.

**Fig. 4.** The spread diameter test.

The cubic samples with dimensions of 150x150x150 mm were prepared to determine the compressive strength of foamed concrete. The samples were tested by TS-EN 12390-3 (TS EN 12390-3 2002). The compressive strength test is presented in Fig. 5. The samples were kept in the mold for 16 hours and were then placed in curing pools at 20 °C. Compressive strength test samples were tested at the end of 7 and 28-day cures.

**Fig. 5.** The compressive strength test.

Prismatic samples measuring 40x40x160 mm were prepared for the flexural test. The samples were tested according to the TS-EN 12390-5 (TS EN 12390-5 2019), as seen in Fig. 6. The density of foam concrete was measured according to TS-EN 12390-7 (TS-EN-12390-7 2010).

**Fig. 6.** The flexural strength test.

## 3. Results and Discussion

A mini slump test was applied to evaluate the workability of samples prepared according to different sisal fiber ratios. Foam concrete was filled into the cylindrical mold with a height and diameter of 80 mm. The cylindrical mold was then removed to allow the foamed concrete to spread. After the foam concrete became stable, the spreading diameter was measured. Workability in foam concrete is affected by many parameters (amount and type of foaming agent, amount of fiber, water/cement ratio, etc.) (Amran et al. 2015; Kearsley and Mostert 2005; Nambiar and Ramamurthy 2006; Rooholamini et al. 2018). Increasing the amount of fiber in foam concrete increases stability, as workability decreases (Yildizel 2020). Increasing the fiber ratio in the mixture increases the internal resistance of the mixture. Therefore, while the stability in the mixture increases, the fluidity decreases. Additionally, there is a decrease in workability due to natural fibers absorbing water. Mini slump test results are presented in Fig. 7. The increase in the amount of fiber causes the spreading diameter to decrease. However, while the loss in workability was less in samples containing 0.25% and 0.50% fiber, the workability decreased more in samples containing 0.75% and 1.00% fiber. The results are consistent with the literature (Calis et al. 2021; Gencel et al. 2022; Hanafi et al. 2020).

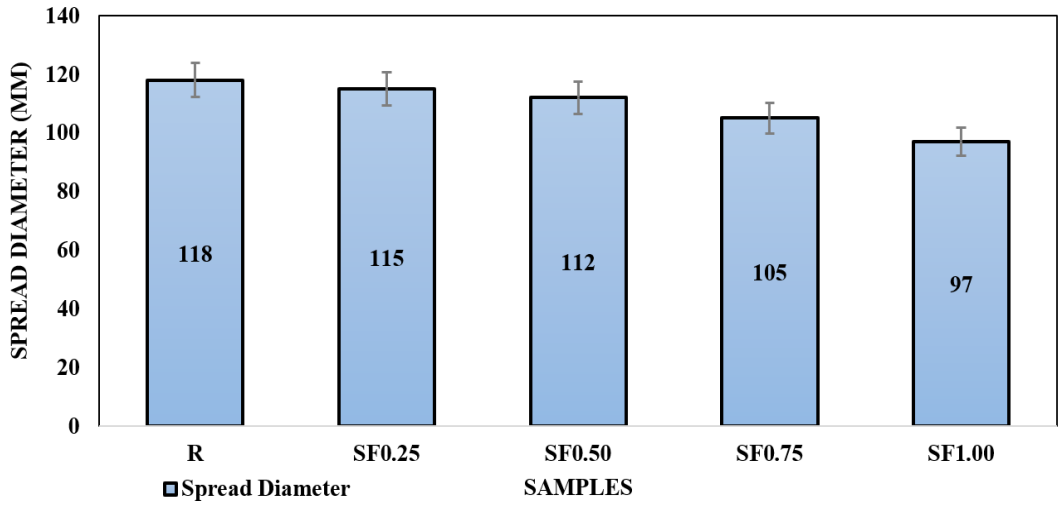


**Fig. 7.** The mini-slump test results.

The change in density in fiber-added foam concrete depends on the amount of fiber. Increasing the amount of fiber causes the number of solids in the mixture to increase. The increase in the number of solids increases the density of concrete (Mydin et al. 2023). In this study, it was observed that the density increased in samples with an increasing fiber ratio. In addition, increasing the fiber ratio may cause changes in the foam structure in the concrete. Fibers in concrete can affect the stability and size distribution of air bubbles, causing the density of the concrete to change. Deterioration of the foam structure causes the density of the concrete to increase. Fresh and hardened foam concrete densities are given in Fig. 8. The increase in fiber content caused the density of foam concrete to increase. The increase in the amount of fiber increased the amount of solid matter in the mixture, causing the density to increase slightly. However, the difference was not significant.

The compressive strengths of the samples depending on different fiber ratios are presented in Fig. 9 for 7 and 28 days. The highest compressive strength was obtained in the sample with a fiber content of 0.50%. The compressive strength of SF0.50 increased by 12.9% compared to the reference sample. Foamed concrete mechanical properties depend on the concrete matrix and the microstructure of the concrete. Adding fiber to the concrete matrix increased the compressive strength of foam concrete. In fiber-added foam concrete, fibers contribute to the concrete compressive strength by reducing crack propagation (Mahzabin et al. 2018; Serri et al. 2014). In addition, the fibers caused the air bubbles in the foam concrete to break down, thus reducing the voids in the concrete. This also contributed to the increase in compressive strength in foam concrete (Yildizel and Calis 2019). Fiber content greater than 0.50% caused the foam concrete strength to decrease.

The reason for this is that the hydration water decreases as a result of the fibers absorbing the water in the concrete. The large surface area of the fibers increases their water absorption (Farzanian et al. 2016; Pourjavadi et al. 2013). Hydration water was insufficient due to the amount of fiber in the mixture being more than a certain ratio. The results are compatible with the literature (Amran et al. 2015; Ardhira et al. 2023).

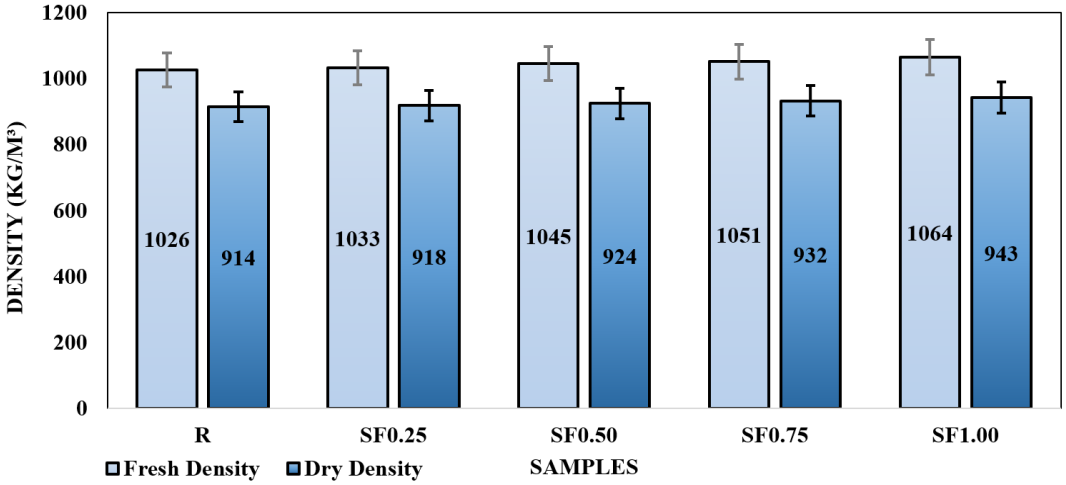


**Fig. 8.** Fresh and dry density values.

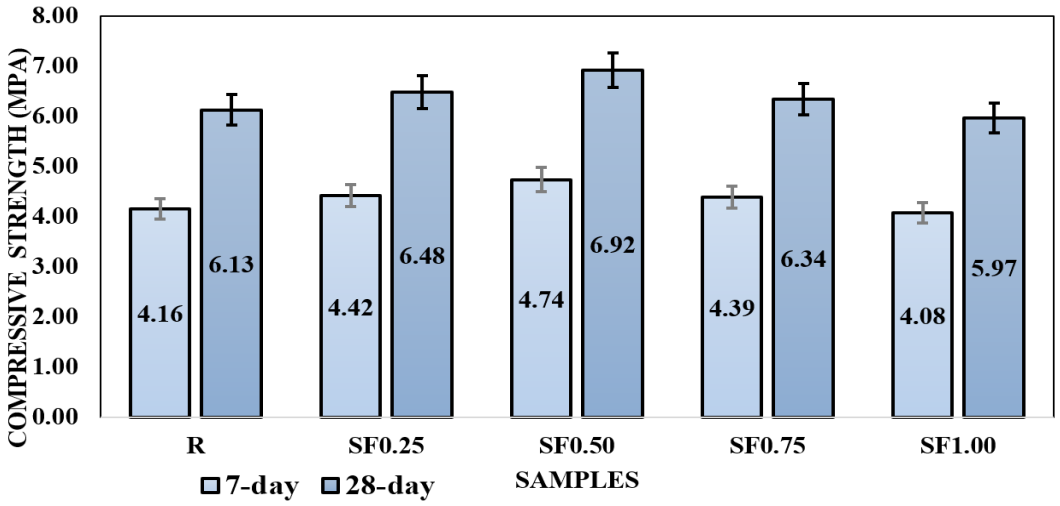


**Fig. 9.** The compressive strength test results.

Flexural strength test results are shown in Fig. 10. While the increase in the amount of fiber increased the flexural strength up to a certain ratio, more than a certain ratio caused the strength to decrease. The highest flexural strength was obtained in the SF0.50 sample. The flexural strength of the SF0.50 sample is 2.85 times higher than the reference sample. Due to the high tensile strength of sisal fibers, adding them to concrete at a certain ratio increases flexural strength (Castillo-Lara et al. 2020; Raj et al. 2020). Fiber content greater than 0.50% caused a decrease in strength. Using more than a certain amount affects the distribution of fibers in the mixture due to the increase in fiber concentration (Raj et al. 2020).

Although the increase in fiber amount causes the fiber distribution in the matrix to deteriorate, even SF0.75 and SF1.00 samples have more flexural strength than the reference sample. Due to the high tensile strength of sisal fiber, it improves the flexural strength of concrete compared to the reference sample even when used in high amounts. Because the flexural strength of conventional concrete is quite weak. Natural fibers, especially sisal fiber, have very high water absorption. Therefore, it absorbs the hydration water in the concrete. Decreasing hydration water reduces the ultimate strength of concrete. Therefore, the use of high fiber reduces flexural strength. To use high amounts of fiber, the surface of the fibers should be coated.

## 4. Conclusions

In this study, the properties of sisal fiber-added foam concrete were examined. The foamed concrete samples with different sisal fiber ratios were prepared. Workability was evaluated for each mixture. The mechanical properties of the samples were examined. The findings obtained based on the test results are as follows:

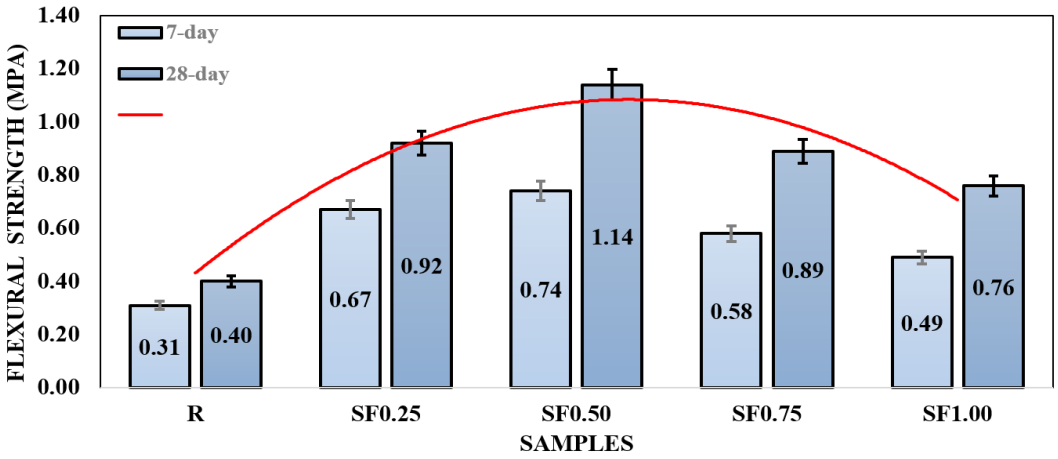


**Fig. 10.** The flexural strength test results.

- Sisal fiber improved the compressive strength of foam concrete due to its uniform distribution in the concrete matrix. An increase in the amount of sisal fiber up to 0.50% increased the compressive strength of foam concrete. The use of more than %0.50 sisal fiber reduced the compressive strength as it greatly increased the concentration within the concrete matrix.
- Approximately a 12.9% increase in compressive strength was achieved in samples using 0.50% sisal fiber. In addition, there were no significant losses in the workability of samples added %0.50 sisal fiber.
- Sisal fiber with high tensile strength contributed to the flexural strength of foam concrete. However, the use of more than 0.50% sisal fiber decreased flexural strength.
- In samples with 0.50% sisal fiber added, the flexural strength increased 2.85 times compared to the reference sample.
- Excessive use of sisal fiber absorbs the hydration water in the concrete. Therefore, the sisal fibers should be coated with waterproof materials to use large amounts of sisal fiber in concrete mixture. There are many surface coating methods such as polyester resin and bio-based shellac. Before these coating methods, some treatment methods can be applied to clean the fiber surface from organic substances. There are many treatment methods recommended in the literature, such as hornification, alkaline treatment and polymer impregnation.
- Even if the workability decreases in foam concretes with sisal fiber addition, the use of 0.50% or fewer sisal fibers provides acceptable workability.
- Foam concrete is used as a non-structural member in buildings with its high heat and sound insulation properties. If the mechanical properties obtained in fiber-added foam concrete are improved, it will also be possible to use it as a structural member.

Foam concrete is preferred in non-structural elements because of its lightweight and high sound and thermal insulation properties. However, its mechanical properties are not sufficient for use as a structural element. Future studies should aim to improve the mechanical properties of foam concrete without increasing its density. In this way, it will be possible to use foam concrete as structural elements.

***Acknowledgements***
*None declared.*

***Funding***
*The author received no financial support for the research, authorship, and/or publication of this manuscript.*

***Conflict of Interest***
*The author declared no potential conflicts of interest with respect to the research, authorship, and/or publication of this manuscript.*

***Data Availability***
*The datasets created and/or analyzed during the current study are not publicly available, but are available from the corresponding author upon reasonable request.*

## REFERENCES

Ahmad J, Majdi A, Deifalla AF, Ben Kahla N, El-Shorbagy MA (2022). Concrete reinforced with sisal fibers (SSF): Overview of mechanical and physical properties. *Crystals*, 12(7), 952.

Amran YHM, Farzadnia N, Abang Ali AA (2015). Properties and applications of foamed concrete; a review. *Construction and Building Materials*, 101, 990–1005.

Ardhira PJ, Ardra R, Harika M, Sathyan D (2023). Study on fibre reinforced foam concrete-a review. *Materials Today: Proceedings*, In Press.

Calis G, Yildizel SA, Erzin S, Tayeh BA (2021). Evaluation and optimisation of foam concrete containing ground calcium carbonate and glass fibre (experimental and modelling study). *Case Studies in Construction Materials*, 15, e00625.

Canbaz M, Bensaoud M, Erol H, Şenge, H (2022). Effect of carbon fibers on the mechanical properties of steam-cured concrete. *Challenge Journal of Structural Mechanics*, 8(2), 38-46.

Castillo-Lara JF, Flores-Johnson EA, Valadez-Gonzalez A, Herrera-Franco PJ, Carrillo JG, Gonzalez-Chi PI, Li QM (2020). Mechanical properties of natural fiber reinforced foamed concrete. *Materials*, 13(14), 3060.

Coutts RSP, Ni Y (1995). Autoclaved bamboo pulp fibre reinforced cement. *Cement and Concrete Composites*, 17(2), 99–106.

Çakıroğlu C, Bekdaş G (2021). Buckling analysis of natural fiber reinforced composites. *Challenge Journal of Structural Mechanics*, 7(2), 58-63.

Falliano D, De Domenico D, Ricciardi G, Gugliandolo E (2018). Experimental investigation on the compressive strength of foamed concrete: Effect of curing conditions, cement type, foaming agent and dry density. *Construction and Building Materials*, 165, 735–749.

Farzanian K, Pimenta Teixeira K, Perdigão Rocha I, De Sa Carneiro L, Ghahremaninezhad A (2016). The mechanical strength, degree of hydration, and electrical resistivity of cement pastes modified with superabsorbent polymers. *Construction and Building Materials*, 109, 156–165.

Frydrych M, Hýsek Š, Fridrichová L, Le Van S, Herclík M, Pechočiaková M, Le Chi H, Louda P (2019). Impact of flax and basalt fibre reinforcement on selected properties of geopolymer composites. *Sustainability*, 12(1), 118.

Gencel O, Nodehi M, Yavuz Bayraktar O, Kaplan G, Benli A, Gholampour A, Ozbakkaloglu T (2022). Basalt fiber-reinforced foam concrete containing silica fume: An experimental study. *Construction and Building Materials*, 326, 126861.

Gultekin A (2023). Effect of hemp and basalt fiber on fracture energy of cement-based composites: a comparative study. *Challenge Journal of Concrete Research Letters*, 14(4), 107-117.

Hamada HM, Shi J, Abed F, Humada AM, Majdi A (2023). Recycling solid waste to produce eco-friendly foamed concrete: A comprehensive review of approaches. *Journal of Environmental Chemical Engineering*, 11(6), 111353.

Hanafi M, Aydin E, Ekinci A (2020). Engineering properties of basalt fiber-reinforced bottom ash cement paste composites. *Materials*, 13(8), 1952.

Huang Z, Zhang T, Wen Z (2015). Proportioning and characterization of Portland cement-based ultra-lightweight foam concretes. *Construction and Building Materials*, 79, 390–396.

Ji R, He Y, Zhang Z, Liu L, Wang X (2015). Preparation and modeling of energy-saving building materials by using industrial solid waste. *Energy and Buildings*, 97, 6–12.

Jones MR, McCarthy A (2005). Preliminary views on the potential of foamed concrete as a structural material. *Magazine of Concrete Research*, 57(1), 21–31.

Kearsley EP, Mostert HF (2005). Designing mix composition of foamed concrete with high fly ash contents. *Proceedings of the International Conference on the Use of Foamed Concrete in Construction*.

Mahzabin MS, Hock LJ, Hossain MS, Kang LS (2018). The influence of addition of treated kenaf fibre in the production and properties of fibre reinforced foamed composite. *Construction and Building Materials*, 178, 518–528.

Mydin MAO, Abdullah MMAB, Hamah Sor N, Omar R, Dulaimi A, Awoyera PO, Althoey F, Deifalla AF (2023). Thermal conductivity, microstructure and hardened characteristics of foamed concrete composite reinforced with raffia fiber. *Journal of Materials Research and Technology*, 26, 850–864.

Naik TP, Gairola S, Singh I, Sharma AK (2024). Microwave-assisted alkali treatment of sisal fiber for fabricating composite as non-structural building materials. *Construction and Building Materials*, 411, 134651.

Nambiar EKK, Ramamurthy K (2006). Influence of filler type on the properties of foam concrete. *Cement and Concrete Composites*, 28(5), 475–480.

Netinger Grubeša I, Marković B, Gojević A, Brdarić J (2018). Effect of hemp fibers on fire resistance of concrete. *Construction and Building Materials*, 184, 473–484.

Okeola A, Abuodha S, Mwero J (2018). Experimental investigation of the physical and mechanical properties of sisal fiber-reinforced concrete. *Fibers*, 6(3), 53.

Oren OH, Gholampour A, Gencel O, Ozbakkaloglu T (2020). Physical and mechanical properties of foam concretes containing granulated blast furnace slag as fine aggregate. *Construction and Building Materials*, 238, 117774.

Pourjavadi A, Fakoorpoor SM, Hosseini P, Khaloo A (2013). Interactions between superabsorbent polymers and cement-based composites incorporating colloidal silica nanoparticles. *Cement and Concrete Composites*, 37, 196–204.

Raj A, Sathyan D, Mini KM (2019). Physical and functional characteristics of foam concrete: A review. *Construction and Building Materials*, 221, 787–799.

Raj B, Sathyan D, Madhavan MK, Raj A (2020). Mechanical and durability properties of hybrid fiber reinforced foam concrete. *Construction and Building Materials*, 245, 118373.

Renjith PK, Sarathchandran C, Sivanandan Achary V, Chandramohanakumar N, Sekkar V (2021). Micro-cellular polymer foam supported silica aerogel: Eco-friendly tool for petroleum oil spill cleanup. *Journal of Hazardous Materials*, 415, 125548.

Rooholamini H, Hassani A, Aliha MRM (2018). Evaluating the effect of macro-synthetic fibre on the mechanical properties of roller-compacted concrete pavement using response surface methodology. *Construction and Building Materials*, 159, 517–529.

Sabarish KV, Paul P, Bhuvaneshwari, Jones J (2020). An experimental investigation on properties of sisal fiber used in the concrete. *Materials Today: Proceedings*, 22, 439–443.

Serri E, Suleiman MZ, Mydin MAO (2014). The effects of oil palm shell aggregate shape on the thermal properties and density of concrete. *Advanced Materials Research*, 935, 172–175.

Shaheen Y, Etman Z, Kandil D (2023). Performance of light weight ferrocement composite walls. *Challenge Journal of Concrete Research Letters*, 14(3), 69-88.

Shalwan A, Alajmi M, Alajmi A (2017). Insulation characteristics of sisal fibre/epoxy composites. *International Journal of Polymer Science*, 2017, 1–6.

Shi J, Liu B, He Z, Liu Y, Jiang J, Xiong T, Shi J (2021). A green ultra-lightweight chemically foamed concrete for building exterior: A feasibility study. *Journal of Cleaner Production*, 288, 125085.

Tran NP, Nguyen TN, Ngo TD, Le PK, Le TA (2022). Strategic progress in foam stabilisation towards high-performance foam concrete for building sustainability: A state-of-the-art review. *Journal of Cleaner Production*, 375, 133939.

TS-EN-197-1 (2000). Cement–Composition, Specifications and Conformity Criteria–Part 1: Common Cements. Turkish Standard Institute, Ankara, Türkiye.

TS-EN-1170-1 (1999). Precast concrete products–Test method for glass-fibre reinforced cement–Part 1: Measuring the consistency of the matrix "Slump test" method. Turkish Standard Institute, Ankara, Türkiye.

TS EN 12390-3 (2002). Testing hardened concrete–Part 3: Compressive strength of test specimens. Turkish Standard Institute, Ankara, Türkiye.

TS EN 12390-5 (2019). Testing hardened concrete–Part 5: Flexural strength of test specimens. Turkish Standard Institute, Ankara, Türkiye.

TS-EN-12390-7 (2010). Testing hardened concrete–Part 7: Density of hardened concrete. Turkish Standard Institute, Ankara, Türkiye.

Wang W, Zhang Y, Mo Z, Chouw N, Jayaraman K, Xu Z (2023). A critical review on the properties of natural fibre reinforced concrete composites subjected to impact loading. *Journal of Building Engineering*, 77, 107497.

Yildizel SA (2020). Material properties of basalt-fiber-reinforced gypsum-based composites made with metakaolin and silica sand. *Mechanics of Composite Materials*, 56(3), 379–388.

Yildizel SA, Calis G (2019). Design and optimization of basalt fiber added lightweight pumice concrete using Taguchi method. *Revista Romana de Materiale/ Romanian Journal of Materials*, 49(4), 544–553.

Zhang A, Liu K, Li J, Song R, Guo T (2024). Static and dynamic tensile properties of ultra-high performance concrete (UHPC) reinforced with hybrid sisal fibers. *Construction and Building Materials*, 411, 134492.

Zini E, Scandola M (2011). Green composites: An overview. *Polymer Composites*, 32(12), 1905–1915.

Challenge Journal of Concrete Research Letters

Research Article

# Investigation of the seismic response of irrigation channel using Coupled Eularian-Lagrangian approach

Muhammet Ensar Yiğit [a], Betül Üstüner [a,*]

[a] *Department of Civil Engineering, Manisa Celal Bayar University, 45140 Manisa, Türkiye*

**ABSTRACT**

While devastating earthquakes affect cities, they can also cause serious damage to irrigation structures in agricultural areas. Cracks and structural deteriorations may occur in water structures using concrete such as dams, aqueducts and open channels. This study investigates the earthquake response of irrigation canals through fluid-structure interaction analysis. The earthquake response of an irrigation canal was examined by establishing fluid-structure interaction. Finite element models, with material properties and dimensions determined, were created and analysed with destructive earthquake records. In the finite element model, the behaviour of water inside the channel is simulated using the Coupled Eulerian-Lagrangian (CEL) approach. In the analyses, displacement and stress values were examined in the model without water, and in addition to these, fluctuations on the water surface were examined in the model with water. The observed changes are shown with graphs and contour diagrams. As a result, it was shown that hydrodynamic effects reduced horizontal displacements by 42% but increased the maximum principal tensile stresses by 49% and the maximum principal compressive stresses by 75%, compared to the non-water model. In addition, it was observed that in both models, the dynamic analysis values at the time of the earthquake increased by approximately 7–13 times the static values before the earthquake. These findings underscore the importance of dynamic analysis using fluid-structure interactive models for safeguarding irrigation structures against seismic hazards, thereby ensuring food security in vulnerable agricultural regions. Therefore, it is important to perform dynamic analysis with fluid-structure interactive models for irrigation structures exposed to destructive earthquake forces.

**ARTICLE INFO**

*Article history:*
Received 4 April 2024
Revised 29 April 2024
Accepted 10 May 2024

*Keywords:*
Fluid mechanics
Hydromechanics
Irrigation canals
Numerical modelling
Structural dynamics



## 1. Introduction

Today, the world's population is rapidly increasing, and this situation is exerting significant pressure on the management of water resources. While the growing population increases the demand for water, the fact that water resources are limited makes water management more critical. In this context, the sustainable use and distribution of water is becoming increasingly important (Cosgrove and Loucks 2015; Sophocleous 2004). Water management involves the effective use, distribution and conservation of water. With the increasing population, there are increases in water consumption areas such as agricultural irrigation, industrial use and urbanization. The growing population and urbanization have driven a rapid expansion in the construction sector (Canbaz et al. 2021). While this situation requires more efficient use of water resources, it also requires the development of sustainable water resources management strategies. Management of water resources includes distributing water equitably, reducing the risks of water scarcity, and protecting water resources (Jury and Vaux 2007; Pedro-Monzonís et al. 2015). With the increasing population, using water resources more efficiently and protecting them for future generations becomes even more important. As a result, while the increasing population

* *Corresponding author*. Tel.: +90-236-201-2301 ; E-mail address: betul.celik@cbu.edu.tr (B. Üstüner)
ISSN: 2548-0928 / DOI: https://doi.org/10.20528/cjcrl.2024.03.003

makes water management more important, strategic planning and implementation is required to effectively use and protect water resources. In this context, sustainable water management policies and projects are vital to meet the water demand of the increasing population and to transfer water resources to future generations. Channels constitute an important part of irrigation systems and are structural elements that enable the distribution of water to irrigate agricultural lands (Angelakıs et al. 2020; Ertsen 2010). These canals are usually placed on prefabricated legs and are generally built-in rows with 5-to-7-meter intervals. The observation and laboratory tests conducted to examine the current condition of the ducts made between 1960–1966 were crucial. In these tests, carried out in laboratories, important characteristics such as weld strength, tensile strength, yield point, and elongation at break were examined. As a result of these tests, it was determined that the ducts produced were suitable for prefabricated structures (Uluöz and Tayakısı 2003). Such tests are essential for determining the quality and performance of building materials and are widely used in the construction industry to ensure reliability. The outcome of these tests indicates how reliable a particular material is under certain conditions, thereby helping to determine its suitability. Channels are the basic building blocks of the flume and allow water to flow in a certain direction. Flumes are generally arranged prefabricated and designed as small water channels. Generally, their cross-section can be elliptical or circular (Fig. 1). An important feature of these flumes is that the water level can be kept at the desired level by changing the foot heights. In this way, the slope of the channel is adjusted to ensure that the water remains at the desired level. This adjustment is made depending on irrigation requirements and the topography of the land. These channels are used to provide water to farmers according to the water demand system or unit field unit water system to meet irrigation needs. These systems ensure the effective distribution of water and regular irrigation of agricultural lands. In addition, balanced distribution of water increases agricultural productivity by meeting the water needs of plants (Özbek 1987). They are used for various purposes such as directing, storing, transporting or distributing water. Canals are widely used in areas such as agricultural irrigation, drinking water supply, industrial processes, flood control and hydroelectric power generation. These structures contribute to the effective and efficient management of water resources (Vanani and Ostad-Ali-Askari 2022). Canals used for agricultural irrigation support food production by increasing agricultural productivity. Drinking water channels meet the water needs of cities and meet a basic need for a healthy life. Therefore, channel structures are of fundamental importance in water management and infrastructure projects.

**Fig. 1.** Prefabricated irrigation flume samples (URL 1; Sepetçioğlu et al. 2018).

Channel structures offer significant advantages in irrigation systems (Hunt 1988; Zhang et. al. 2019). Since they are prefabricated, construction times are short and material quality is high. In this way, long-lasting and durable structures can be obtained with a quick assembly process. Additionally, it is easy to maintain and repair, reducing operating costs. Since channel structures are built on piers at a certain height from the ground, they are almost unaffected by surface flows. This increases irrigation efficiency and ensures that water reaches the plants directly. Since their sealing properties are higher, they can be transported and reused. Routes can be easily changed by disassembly, which provides flexibility. Since the water level is kept high thanks to the feet, it provides ease of irrigation and there is no need for sockets. In addition, channel structures take up little space, which reduces their costs. Since the legs are high enough, it prevents weeds from growing. Additionally, the small water surface reduces evaporation and increases irrigation efficiency. As a result, channel structures offer many advantages such as fast installation, low maintenance costs, durability, flexibility and increased irrigation efficiency. These structures increase agricultural productivity and support the sustainable use of water resources by ensuring the effective and efficient use of water.

Canal irrigation networks may encounter some disadvantages in some cases. Canals may not be economical, especially if the irrigation area requires deep drainage. Excavation soils from drainage channels cannot be utilized because there are no tertiary channels, and this may cause additional costs. The number of flumes required for small irrigation fields may not be economical, and remote material transportation may also increase costs. Level errors may occur during construction, which may cause overflows to occur. Additionally, even a single canal falling or breaking along the canal line can cause

irrigation to be interrupted or disrupted. Construction costs increase on sloping lands, which increases the cost of canal irrigation networks. This may lead to additional costs compared to piped irrigation networks. Flume irrigation networks can also be difficult to maintain and repair, which can increase operating costs. Therefore, depending on the irrigation needs and the structure of the land, alternative irrigation methods should also be considered (Sepetçioğlu et al. 2018).

Damages to flume structures are problems that may occur due to various factors. Physical breaking or damage to drains can reduce the efficiency of the irrigation system (Fig. 2). These fractures can be caused by a variety of reasons, such as ground movements, overloading, root pressure or natural disasters. Water leaks may occur at the junctions of drains or structural weak points. These leaks can cause loss of irrigation water and environmental erosion. Mud, sediment or plant debris accumulating in drains can cause blockages. These blockages block the flow of water and can render the irrigation system ineffective. Drains losing their slope over time can make it difficult to keep the water at the desired level. This can reduce irrigation efficiency and cause inadequate water delivery. Drains require regular maintenance. Mud, sediment or plant residues accumulated on the surface should be cleaned and structural damages should be corrected. Otherwise, the performance of the channels may decrease and the irrigation system may become inefficient. In addition, channel structures may be affected by various natural disasters, which may cause various damages. Sewer structures may face floods due to heavy rains. Excessive pressure of high flow water on the channel may cause cracks or erosion on the channel walls due to the corrosive effect of the water. Earthquakes can cause serious damage to channel structures. Cracks, bending or ruptures may occur in the channels due to ground shifts or direct structural weaknesses. Heavy rains or floods can cause landslides in the soil around canal structures. This can weaken the supports of the channel piers, damaging the structure. In cold climates, the freezing-thawing cycle of water in channel structures can cause expansion and contraction in the structural elements. This may cause cracks to form in the channel walls and deteriorate structural integrity. Severe storms and hurricanes can directly damage channel structures. The pressure applied to the channel walls due to the intensity of the wind may cause damage or dislocation of the channel elements. Flooding resulting from heavy rains or overflow of water resources can cause serious effects on channel structures. A sudden increase in water height can cause erosion, erosion and collapse of channel walls. Channel designs that are resistant to these natural disasters can ensure less damage to structures. Regular maintenance, damage assessment and strengthening works can also increase the durability of channel structures and strengthen their resistance to natural disasters (Sepetçioğlu et al. 2018).

**Fig. 2.** Damages occurring in various irrigation channel:
(a) Manisa; (b) Hasandede/Kırıkkale; (c) Kahramanmaraş (URL 2; URL 3).

Canal irrigation networks are prefabricated channels and generally consist of saddles, foundations and foundation blocks. Farmers irrigate through portable siphons placed inside the sewers. In canalized irrigation networks, there are no drainage tertiaries in the classical system. However, the drainage backup and main drainage channel are also planned according to the same principles. It consists of main structural elements such as channel, prefabricated flooring, retaining saddle, foundation and foundation block (Fig. 3.). These channels are placed on prefabricated legs of different heights, and the water is kept at the desired level by changing the foot heights (Xiao and Wu 2022).

Channel structures have an important place in irrigation systems and are important structural elements that ensure the effective distribution of water. These structures are of critical importance for irrigation of agricultural areas and management of water resources. Nowadays, studies on these structures are becoming increasingly important. Bayramoğlu (2006) aimed to select an economically and technically suitable network in the Küre-Katlıç, Selbüküköy and Gemiciköy regions of the Central Sakarya Basin Irrigation by DSI (Republic of Türkiye, General Directorate of State Hydraulic Works). In his study, he discussed the importance of channel structures and their intended use in social and economic terms. The suitability of the network systems chosen instead of these systems with today's technology was examined. Aydoğdu (2006), in his study on the evaluation of water resources and irrigation-drainage systems, presented suggestions on management and business issues that will ensure optimum use of resources, institutional

and legal contents, social and cultural behaviors, environmental interaction potential, financial and economic needs. He compared other irrigation systems and talked about the advantages and disadvantages of flume structures. Sarı (2010) discussed the Balıkesir and Gönen Plains Irrigation in Balıkesir province in his thesis study. The data from the flume structures between 2005 and 2009 were evaluated using the linear regression analysis method, and the problems encountered during operation and irrigation efficiency were examined. Aydoğdu and Yenigün (2008) conducted a comprehensive evaluation of irrigation systems and drainage requirements in projects within the Euphrates and Tigris basins. Their assessment focused on analyzing water resources, irrigation systems, and water distribution methods based on collected data and field observations. Additionally, they identified water control structures and drainage needs.

Furthermore, recommendations were provided to ensure efficient water usage, detect potential operational issues, and prevent similar problems in future projects. These recommendations encompass management and operational strategies to optimize resource utilization, institutional and legal regulations, social and cultural factors, environmental interaction potentials, and economic requirements.

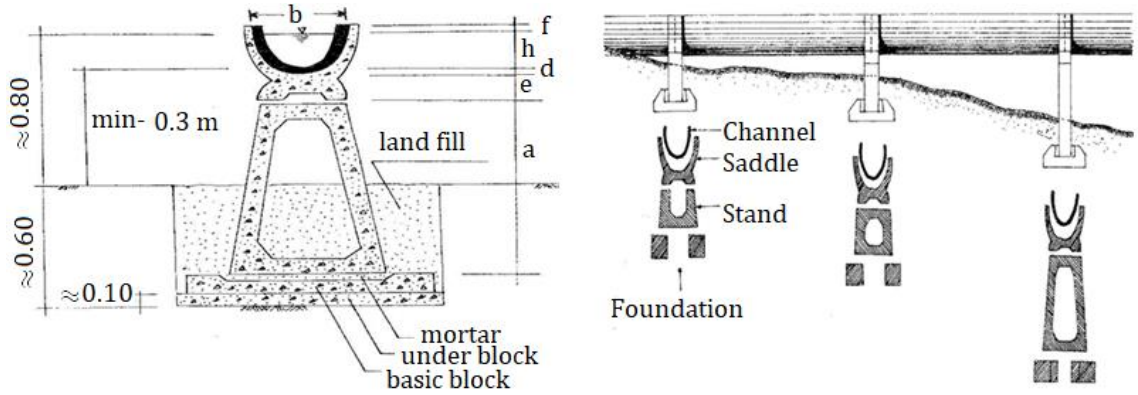


**Fig. 3.** Figure definition: (a) Schematic representation of flume system cross-section; (b) Flume system parts and on-site assembly situation (URL 5).

In this study, studies were carried out using the Coupled Euler-Lagrangian approach to evaluate the seismic responses of channel systems. This approach best represents the fluid-structure interaction and has features not found in other models. For example, it allows the observation of situations such as shaking of the water in the channel, possible overflow and spillage. Material models adapted to different duct units were used in the study. Three different models were analysed using the destructive earthquake record and the results were compared. These studies can be considered as an important step towards improving the seismic performance of channel structures and increasing their safety.

## 2. Coupled Eularian-Lagrangian Analysis for Prefabricated Flume-Fluid Interaction

The Eulerian approach tracks how variables (e.g. velocity, pressure, or temperature) change at a point in the flow at a given time. This approach describes the flow at a specific point and observes the variables at that point over time. In contrast, the Lagrangian description follows the motion of individual particles or elements of a material. With the Lagrangian approach, the motion of a particle (or element) is monitored at a given time and the properties associated with this particle are formulated considering the position and speed of the particle in motion. These two approaches are different but complementary methods for analysing the behaviour of flow (Skrzat 2012). The Coupled Euler-Lagrange approach is a method used in research to study complex interactions and is often used in research on the design, safety and sustainability of water structures and in risk analysis. This method helps make informed decisions regarding the safety, integrity, and risk assessment of structures by considering both the broad spatial context and the behaviour of individual elements (Şermet et al. 2024; Zwick and Balachandar 2020; Martin et al. 2020).

$$\text{Conservation of mass} \quad : \frac{D\rho}{Dt} + \rho \nabla . u = 0 \tag{1}$$

$$\text{Conservation of momentum} \quad : \rho \frac{Du}{Dt} + \nabla . \sigma + \rho \beta \tag{2}$$

$$\text{Conservation of energy} \quad : \frac{D\epsilon}{Dt} = \sigma : D \tag{3}$$

Here, $u$ is the velocity vector, $\rho$ is the density, $\sigma$ is the Cauchy stress, $\beta$ is the body force and e is the rate of internal energy per unit volume. The $D/Dt$ operator is the material derivative operator defined by Eq. (4).

$$\frac{D\psi}{Dt} = \frac{\partial \psi}{\partial t} + u . \nabla \psi \tag{4}$$

The $\psi$ in the equation represents an arbitrarily chosen physical quantity. $\nabla$ is a vector and differential operator and is expressed in Cartesian and cylindrical coordinates, respectively, as follows.

$$\nabla = i \frac{\partial}{\partial x} + j \frac{\partial}{\partial y} + k \frac{\partial}{\partial z} \tag{5}$$

$$\nabla = e_r \frac{\partial}{\partial r} + e_\theta \frac{\partial}{\partial y} + e_z \frac{\partial}{\partial z} \quad (6)$$

$\{x, y, z\}$ in Eq. (5) represents Cartesian coordinates, and $\{i, j, k\}$ represents the unit vectors of these coordinates. $\{r, \theta, z\}$ used in Eq. (6) represents cylindrical coordinates, and $\{r, \theta, z\}$ represents the unit vectors of cylindrical coordinates. The general equation of the Euler approximation obtained by using Eq. (5) in the conservation equations:

$$\frac{\partial \psi}{\partial t} + \nabla . \varphi = S \quad (7)$$

It is in the form. $\varphi$ used in the equation: flow function, $S$: source term (Benson and Okazawa 2004; Zhang and Zhang 2014).

## 3. Linear Dynamic Analysis of Prefabricated Irrigation Channel

In this study, a three-dimensional model was built to examine the turbulence occurring during the transverse ground movement of the prefabricated flumes that provide irrigation to the Manisa plain in the central Gediz Basin within the scope of the Demirköprü Dam Irrigation project. The construction of Demirköprü and the hydroelectric power plant started in 1954 and was completed in 1960. The installed power of the power plant, which consists of three units of 23 MW each, is 69 MW. The annual electricity production capacity of the power plant is 193 million kWh. By producing energy, the water coming out of the turbines is taken into channels from the Adala Regulator, approximately 1 km southwest, to irrigate 25000 ha of Adala, 65000 ha of Ahmetli and 22000 ha of Menemen (Gündoğdu and Kocataş, 2006; Güner et al., 2016).

Macro modelling was done in this study. The flume capacity is modelled as 200 lt/h. Flow speed: $V$ = 1 m/s, cross-section wet area: $A$ = 0.2 m$^2$, air share: $f$ = 0.2 m, length: $L$ = 5.0 m, water depth: $h$ = 0.5 m, water surface width: $b$ = 0.5 m (Fig. 4).

### 3.1. Material properties

The concrete flume material was chosen as C20 class and 0.05 m thick concrete. The linear material properties for concrete, steel, and water are provided in Table 1. Mechanical properties of concrete, steel and water were taken from the specified sources in accordance with the literature (Lin and Wu 2016; Yiğit et al. 2019; Yıldızel et al. 2014; Yıldızel 2020; Yılmaz 2023; URL 6).

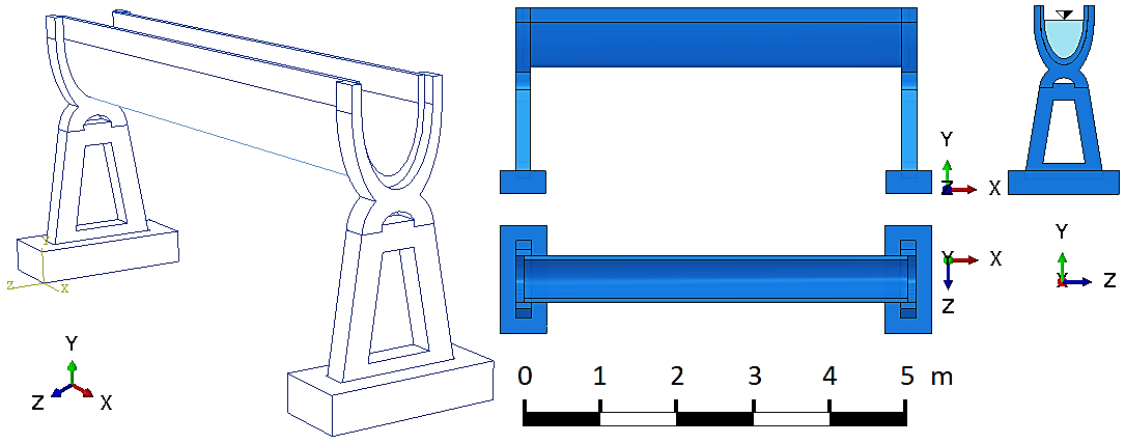


**Fig. 4.** Schematic representation of the flume.

**Table 1.** Concrete, steel and water material properties.

| Material | Density (kg/m$^3$) | Modulus of elasticity (MPa) | Poisson's ratio | Speed of sound (m/s) | Dynamic viscosity (N.s/m$^2$) |
|---|---|---|---|---|---|
| Concrete | 2374 | 28000 | 0.2 | - | - |
| Steel | 7834 | 210000 | 0.2 | - | - |
| Water | 1000 | 2200 (Bulk) | - | 1450 | 1.002x10$^{-3}$ |

### 3.2. Flume finite element model

The flume three-dimensional solid model and finite element model (FEM) were created using the ABAQUS software (ABAQUS 2010) (Fig. 5). In the analysis, an explicit dynamic analysis was conducted using the software. This type of analysis is characterized by its consideration of time-dependent and transient effects, where the response of the structure is computed over small time increments. This approach is particularly suitable for modeling scenarios with rapid changes in loading conditions, such as seismic events or fluid structure interaction.

In our study, in ABAQUS enabled us to accurately capture the behavior of the irrigation canal under seismic forces and evaluate its response in detail. In creating the

FEM, a four-node triangular prism element (C3D4) (Fig. 6a) was used for the foundation structure, and an eight-node reduced integration cubic element (C3D8R) (Fig. 6b.) was used for the foot, saddle, channel and liquid. For reinforcement, two-point linear bar (B31) element type was used (Fig. 6c.). In the finite element analysis program, the interaction between the fluid and the structural elements was selected as a hard contact surface that can transfer pressure in the normal direction, and as a frictional contact surface in the tangential direction. The friction coefficient between the fluid and the structure is accepted as 0.03. The mesh spacing to be used in the FEM analysis of the channel was chosen as 0.05 m (Fig. 5b). The results of the analysis using the specified network range are given under the heading "Results". 10892 solid elements and 23252 node points were used in the waterless model, and 66948 solid elements and 84449 nodal points were used in the aqueous model. As a boundary condition, earthquake acceleration $A_X = A_Y = 0$ in the X and Y directions and $A_Z = acc(t)$ in the Z direction were entered at the base. On the sides, $U_x = 0$ was entered only in the $X$ direction. Gravitational acceleration was entered as -9.81 m/s$^2$ in the $Y$ direction.

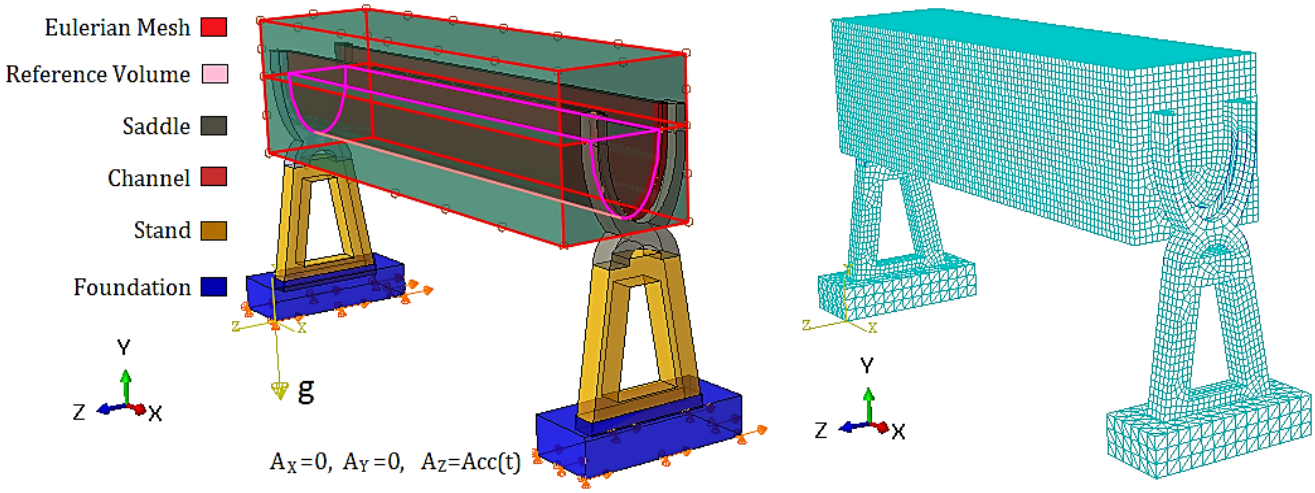


**Fig. 5.** Flume three-dimensional solid model and finite element mesh.

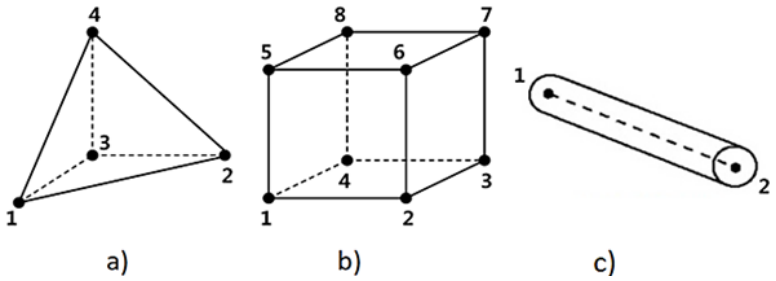


**Fig. 6.** (a) C3D4 triangular prism structural element; (b) C3D8R cube fluid element; (c) B31 linear rod element (ABAQUS 2010).

### *3.3. Seismic records used*

The ground motions corresponding to the main and aftershocks of the earthquakes that occurred in Kahramanmaraş on February 6, 2023, were recorded at several stations operated by Tadas/AFAD. The latitude is 37.4851, the longitude is 37.2978, Vs30 (m/s) is 671, the soil class is ZC, and the effective duration is E-W: 24.07 s, N-S: 23.16 s, U-D: 20.81 s. The distance (Repi) is 61.30 km, and the magnitude (Mw) is 7.7 for the Kahramanmaraş-Pazarcık earthquake. The highest ground acceleration value recorded during this earthquake was at station 4614 in Pazarcık district of Kahramanmaraş province. The value measured in the East-West (E-W) component of the recording was 2.005g, while the North-South (N-S) component was 1.987g, and the vertical (U-D) component was 1.379g. In this study, to observe the fluid's agitation more clearly, the North-South direction, which caused the maximum displacement (approximately 0.23 m), is depicted in Fig. 7 with acceleration-time and spectrum graphs (Tadas 2023). To shorten the analysis time, values of the acceleration record between t=30s and t=70s were used.

## 4. Results and Discussion

The analysis results are presented in three different sections. The first section illustrates the surface shapes of water at different time intervals, showing the agitation of the fluid under the earthquake effect. The second section includes displacement-time graphs of the canal's peak points and the contour diagram depicting the max-

imum relative displacement of the canal. The third section consists of graphs showing the maximum principal tensile-time and maximum principal pressure-time at selected points from the region where the main canal is most stressed, along with contour diagrams corresponding to the maximum stresses of the main canal.

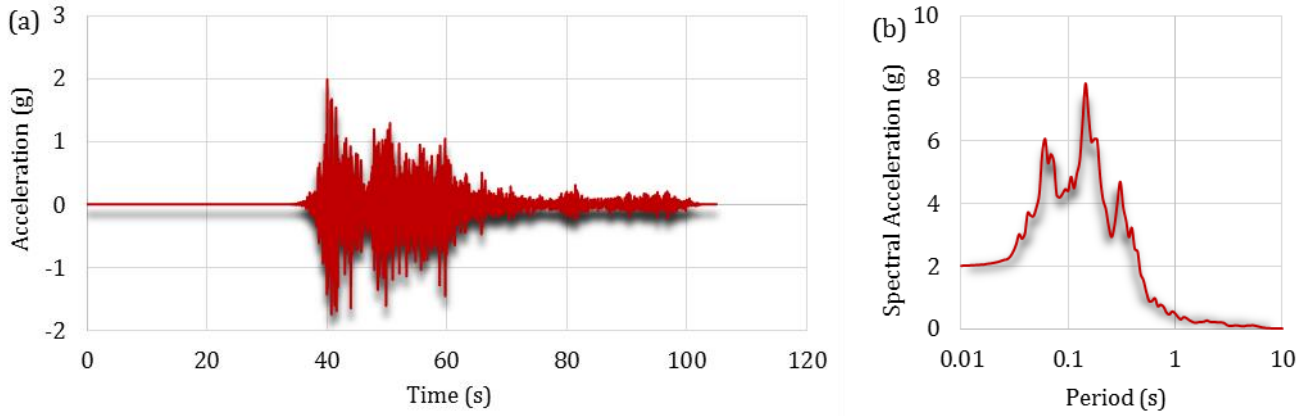


**Fig. 7.** North-South component of the 06/02/2023 Pazarcık/Maraş earthquake: (a) Acceleration-time graph; (b) Spectral acceleration - Period graph.

### *4.1. Flume surface sloshing*

As a result of the sloshing, water surface shapes are magnified by a factor of 5 in the *y-y* direction for different time intervals, as shown in Fig. 8. Upon examining the model, it is observed that the water mass in the canal (shown in blue) has been set in motion and agitated under the earthquake effect. The distance between the wave crest and the wave trough, resulting from this agitation, is measured to be approximately 0.29 meters. The wave height amounted to approximately 58% of the initial water height ($h$=0.50 meters). The total water rise relative to the calm water level is approximately 0.19 meters. This rise accounts for about 40% of the initial water height. It is observed that the previously determined air gap for the canal (0.20 meters) is sufficient.

Since there is no partition wall or porous diaphragm restricting the movement between the fluid and the canal walls in the model, the fluid moves as a whole. Under the earthquake effect, the fluid collides with the canal walls and returns as a whole. This could lead to an increase in the height of the sloshing and overflow outside the canal. These results are consistent with the findings obtained in the literature mentioned in the articles.

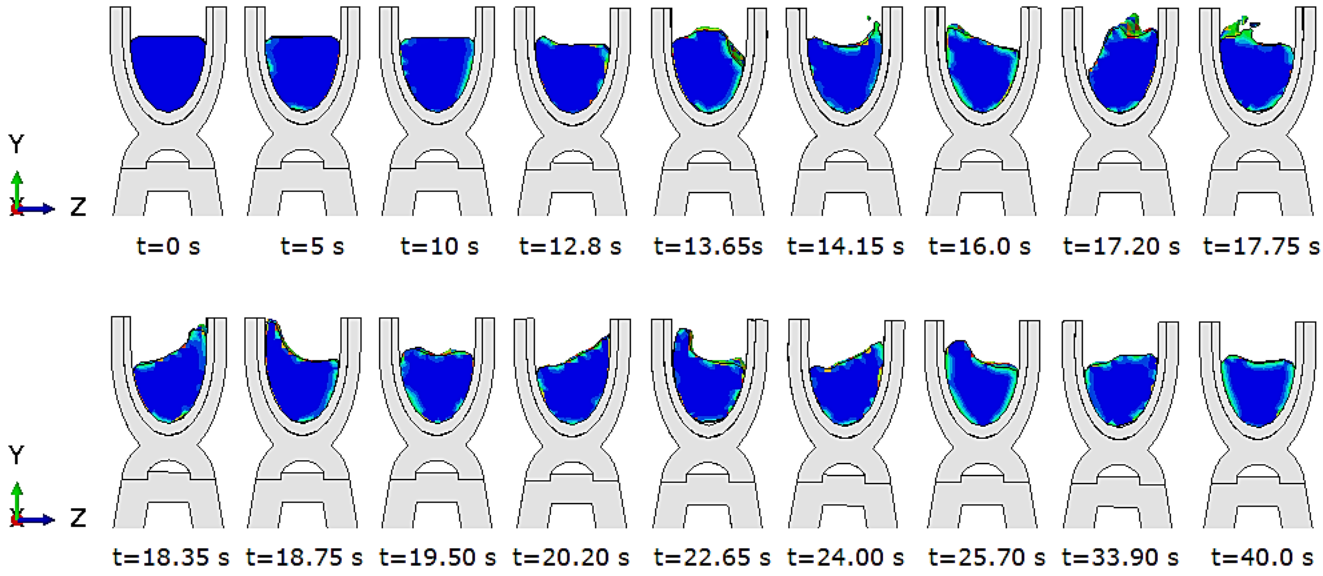


**Fig. 8.** Fluid sloshing surface shapes (CEL model).

Since there is no partition wall or porous diaphragm restricting the movement between the fluid and the canal walls in the model, the fluid moves as a whole. Under the earthquake effect, the fluid collides with the canal walls and returns as a whole. This could lead to an increase in the height of the sloshing and overflow outside the canal. These results are consistent with the findings obtained in the literature mentioned in the articles.

### *4.2. Displacements*

The relative displacement between the top of the flume system and the base in the direction of the earthquake is shown in Fig. 10 as a displacement-time graph.

When Fig. 10 is examined, the maximum relative displacement value at the peak in the empty flume model is 0.087 m, while it is measured as 0.050 m in the water-filled model. The largest relative displacement contour diagrams of both models are given in Fig. 11. As can be seen, the relative displacement in the water-filled model is 42% less than in the empty model. The damping effect of water reduced the horizontal relative displacement values.

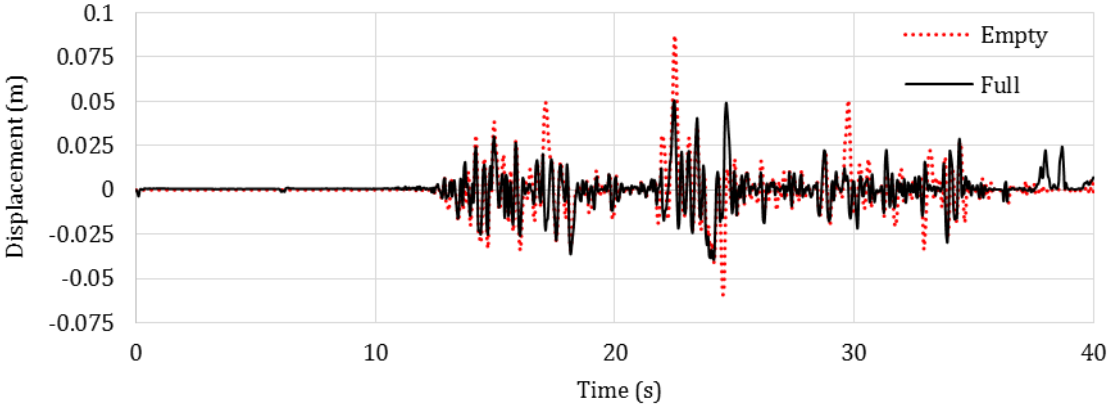


**Fig. 9.** Flume system peak relative displacement-time graph at upper level.

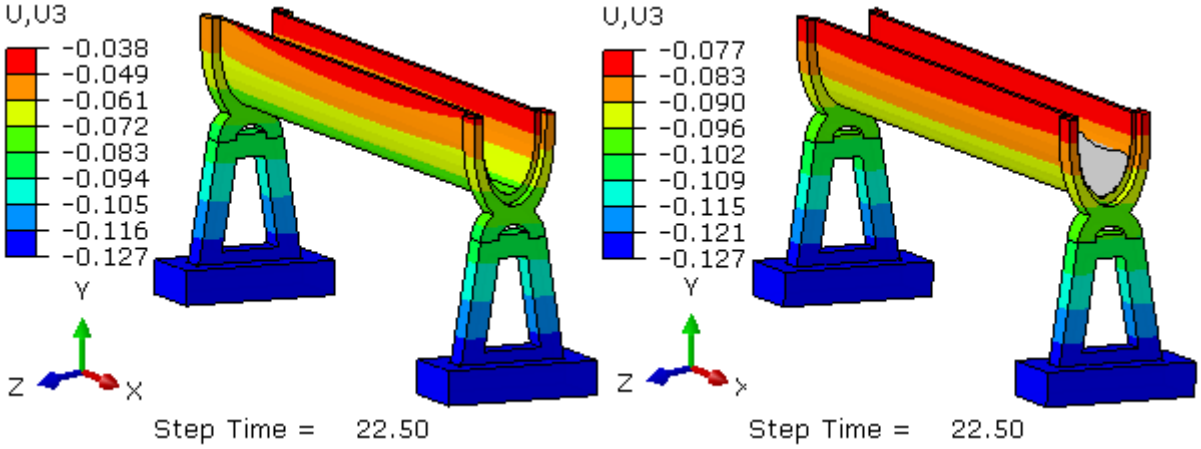


**Fig. 10.** Maximum relative displacement contour diagrams (m):
(a) Flume system empty; (b) Flume system full.

### *4.3. Stresses*

It was predicted that the presence of fluid in the water-filled model would cause an increase in the largest principal tensile stresses and the largest principal compressive stresses. Maximum principal tensile stress-time graphs ($S_{max}$) are given in Fig. 11 and maximum principal tensile stress contour diagrams are given in Fig. 12. As seen in Figs. 11 and 12, the largest principal tensile stresses increased as follows 49% when comparing the empty model with the water-filled model. In addition, in the static situation before the earthquake, the largest principal tensile stresses were measured as 0.48 MPa and 1.42 MPa in the empty and full models, respectively. These values increased to 6.82 MPa and 10.22 MPa due to dynamic effects at the time of the earthquake. This means an increase of approximately 13 times in the empty model and 7 times in the full model. The damping effect of the water in the channel limited the increase in the stress value.

Maximum principal compressive stresses-time graphs ($S_{min}$) and contour diagrams of the greatest principal compressive stresses are given in Figs. 13 and 14. Compared to the empty model, it was observed that the maximum principal compressive stresses increased by 75% in the water-filled model. The largest principal compressive stresses were lowest in the empty model without the additional weight of the fluid. In addition, in the static situation before the earthquake, the largest principal tensile stresses were measured as -0.45 MPa and -1.04 MPa in the empty and full models, respectively. These values increased to -4.98 MPa and -8.61 MPa due to dynamic effects at the time of the earthquake. This means an increase of approximately 11 times in the empty model and 8 times in the full model. The damping effect of the water in the channel limited the increase in the stress value.

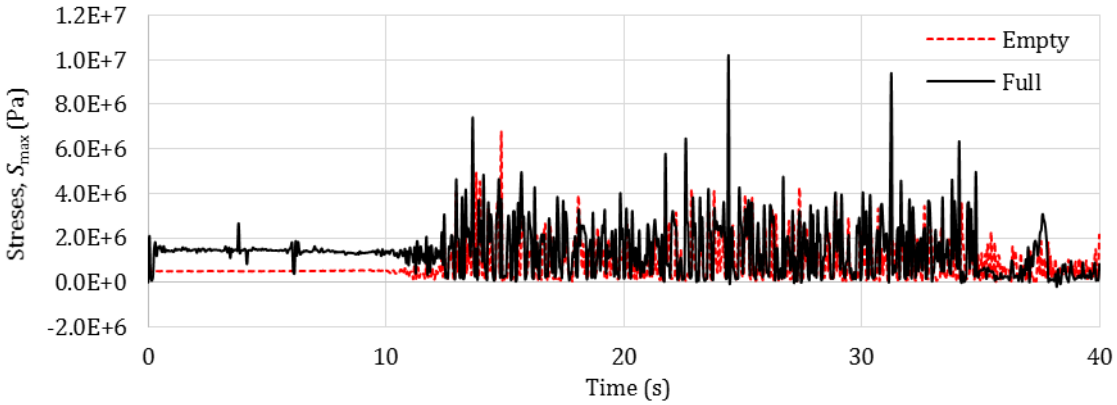


**Fig. 11.** Maximum principal tensile stress-time graphs ($S_{max}$).

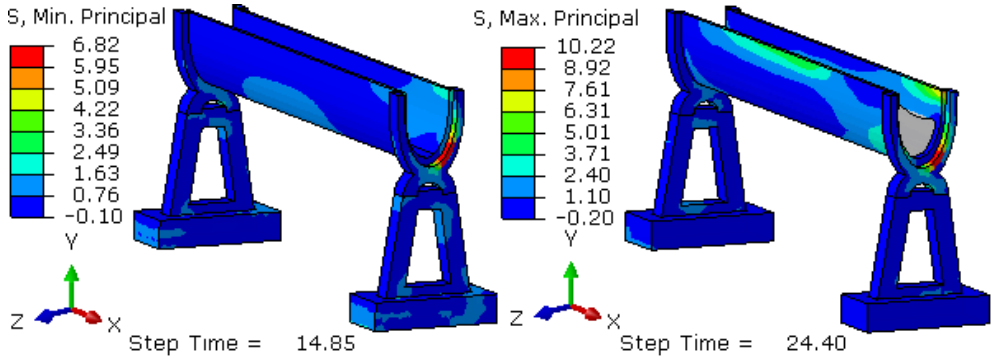


**Fig. 12.** Maximum principal tensile stress contour diagrams (MPa):
(a) Flume system empty; (b) Flume system full.

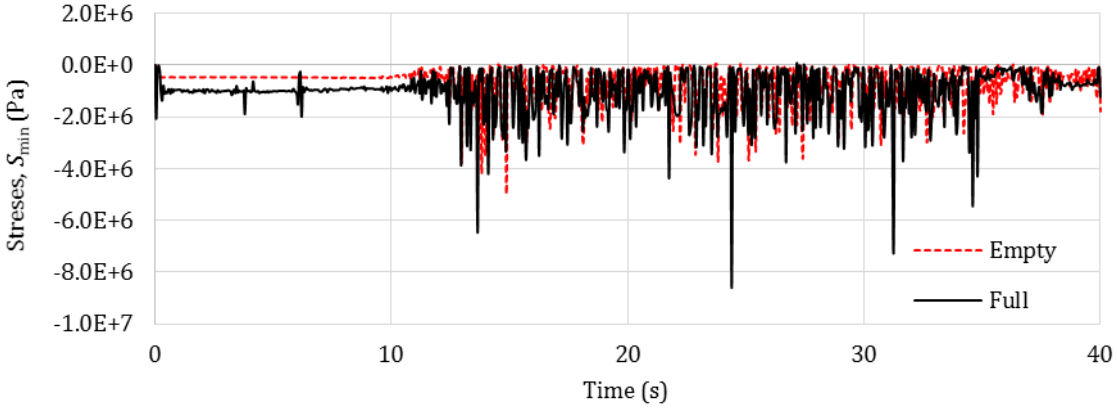


**Fig. 13.** Maximum principal compressive stress-time graphs ($S_{min}$).

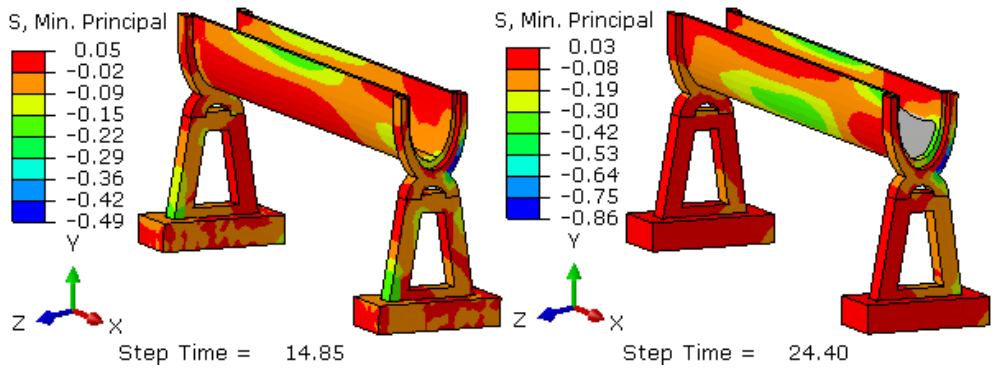


**Fig. 14.** Maximum principal compressive stress contour diagrams (MPa):
(a) Flume system empty; (b) Flume system full.

## 5. Conclusions

In this study, dynamic analysis was carried out to investigate the seismic responses of a prefabricated irrigation canal in its empty and full state. To see the devastating earthquake effects, the North-South record of the 06/02/2023 Pazarcık/Kahramanmaraş earthquake with a Peak Ground Acceleration (PGA) value of approximately 2.0g was used. Water was used as the fluid in the main irrigation channel, the material properties and dimensions of which were taken from the literature. As a result of the analysis, the following results were obtained.

- It has been observed that water turbulence shows earthquake effects with the Coupled Eularian-Lagrangian (CEL) approach. By analysing the models, shaking and possible water overflow during an earthquake could be easily observed.
- During devastating earthquakes, the value between the sloshing peak and trough of the water mass in the prefabricated irrigation canal was approximately 58% of the initial water level, and the water rise was 40% of the initial water level.
- Considering the fluid-structure interaction, relative displacements in the filled model decreased by 42% compared to the empty model.
- The sloshing effect and liquid weight caused an increase of 49% and 75% in the maximum principal tensile stresses ($S_{\max}$) and the maximum principal compressive stresses ($S_{\min}$), respectively.
- In the absence of water, dynamic effects increased the maximum principal compressive stresses by 13 times and the maximum principal tensile stresses by 11 times compared to the pre-earthquake. In the case of water, these increases were 7 times and 8 times, respectively. The damping property of the fluid showed its effect in the case of water.

In all models, the largest principal compressive stress distributions and the largest principal tensile stress distributions are concentrated in an area close to the junction of the base and slope, where the flume is usually damaged in earthquakes.

Future studies that can be done on this subject are listed below as suggestions.

- Prefabricated irrigation channels have different sizes for different flow rates. For this reason, the issue of determining the most appropriate water height and air share under seismic effects can be investigated.
- Fluid-structure interaction seismic analyses can be performed for earthquakes with different PGA(g) values and the results can be compared.
- Comparative analysis can be conducted with different fluid-structure interaction models.
- Analyses can be performed for various fill levels, and the results can be compared.
- The damage situation can be examined in detail by performing nonlinear dynamic analysis of the same structure.

Analyses have shown how the seismic effects of the prefabricated irrigation canal can occur in empty and full situations. For this reason, it is recommended that dynamic calculations and sloshing analysis, as well as static and hydraulic calculations of the main channels, be made by considering the fluid-structure interaction. Thus, floods can be prevented in case of possible earthquakes.

***Acknowledgements***

*None declared.*

***Funding***

*The authors received no financial support for the research, authorship, and/or publication of this manuscript.*

***Conflict of Interest***

*The authors declared no potential conflicts of interest with respect to the research, authorship, and/or publication of this manuscript.*

***Author Contributions***

*All of the authors made substantial contributions to conception and design, or acquisition of data, or analysis and interpretation of data; were involved in drafting the manuscript or revising it critically for important intellectual content; and gave final approval of the version to be published.*

***Data Availability***

*The datasets created and/or analyzed during the current study are not publicly available, but are available from the corresponding author upon reasonable request.*

## REFERENCES

ABAQUS (2010). ABAQUS user's manual, Version 6.10. Dassault Systèmes, SIMULIA.

AFAD (2023). İçişleri Bakanlığı "Afet ve Acil Durum Daire Başkanlığı". [Online]. Available: https://deprem.afad.gov.tr/content/131

Angelakıs AN, Zaccaria D, Krasilnikoff J, Salgot M, Bazza M, Roccaro P, Jimenez B, Kumar A, Yinghua W, Baba A, Harrison JA, Garduno-Jimenez A, Fereres E (2020). Irrigation of world agricultural lands: Evolution through the millennia. *Water*, 12(5), Article 5.

Aydoğdu MH (2006). Evaulation of Water Resources and Irrigation-Drainage Systems of GAP, Southeastern Anatolia Project. *Thesis*, Harran University, Şanlıurfa, Türkiye.

Bayramoğlu E, (2006). Orta Sakarya Havzası Sulama Sahalarındaki Bazı Sulama Hatlarında Dağıtım Şebekesi Seçimi ve Karşılaştırmalı Ekonomik Analizleriyle İlgili bir Çalışma. *M.Sc. thesis*, Anadolu University, Eskişehir, Türkiye.

Benson DJ, Okazawa S (2004). Contact in a multi-material Eulerian finite element formulation. *Computer Methods in Applied Mechanics and Engineering*, 193, 39, 4277–4298.

Canbaz M, Kara İ, Topçu İB (2021). Effect of high temperature on the mechanical behavior of cement-bonded wood composite produced with wood waste. *Challenge Journal of Structural Mechanics*, 7(1), 42-48.

Cosgrove WJ, Loucks DP (2015). Water management: Current and future challenges and research directions. *Water Resources Research*, 51(6), 4823–4839.

Ertsen MW (2010). Structuring properties of irrigation systems: Understanding relations between humans and hydraulics through modeling. *Water History*, 2(2), 165–183.

Gündoğdu V, Kocataş A (2006). Gediz Nehir Havzası Yönetim Planı Oluşturulmasına Yönelik Bir Yaklaşım. *E.U. Journal of Fisheries & Aquatic Sciences*, 23(3-4), 371–378, ISSN 1300 - 1590.

Güner S, Yılmaz OS, Erbaş YS, Gümüş E, Güngör R, Şahbaz K (2016). Demirköprü Barajı'nın Su Kotu Seviyesine göre Arazi Kullanilabilirlik Analizi. *6. Uzaktan Algılama-CBS Sempozyumu* (UZAL-CBS 2016), 5-7 October, Adana, Türkiye.

Hunt RC (1988). Size and the structure of authority in canal irrigation systems. *Journal of Anthropological Research*, 44(4), 335–355.

Jury WA, Vaux HJ (2007). The emerging global water crisis: managing scarcity and conflict between water users. *Advances in Agronomy*, 95, 1–76.

Lin J, Wu Y (2016). Numerical analysis of interfacial bond behavior of externally bonded FRP-to-concrete joints. *Journal of Composites for Construction*, 20, 04016028.

Martin T, Kamath A, Bihs H (2020). A Lagrangian approach for the coupled simulation of fixed net structures in a Eulerian fluid model. *Journal of Fluids and Structures*, 94, 102962.

Özbek T (1987). Sulama Kurutma. Gazi Üniversitesi, Ankara, Türkiye.

Pedro-Monzonís M, Solera A, Ferrer J, Estrela T, Paredes-Arquiola J (2015). A review of water scarcity and drought indexes in water resources planning and management. *Journal of Hydrology*, 527, 482–493.

Sarı T (2010). Balıkesir ve Gönen Ovaları Sulama Sistemlerinin Performanslarının İncelenmesi. *M.Sc. Thesis*, Balıkesir University, Balıkesir, Türkiye.

Sepetçioğlu MY, YeniGün K, Karakuş S, Aslan V (2018). Şanlıurfa ili sulamaları ışığında sulama şebekelerinin karşılaştırılması. *Turkish Journal of Hydraulics*, 2(1), 19-30.

Skrzat A (2012). Application of coupled Eulerian-Lagrangian approach in metal forming simulations. *Mechanika*, 84(4), 25–35.

Sophocleous M (2004). Global and regional water availability and demand: Prospects for the future. *Natural Resources Research*, 13(2), 61–75.

Şermet F, Kartal ME, Yiğit ME, Hökelekli E (2024). The effect of the gravity on the earthquake performance of roller compacted concrete dams. *Challenge Journal of Concrete Research Letters*, 15(1), 20–29.

Uluöz S, Tayakısı A (2003). 1960–1966 yılları arasında üretilerek sulama şebekelerinde kullanılan prefakrik kanaletlerin 2000 yıllındaki mevcut kalitesi. *TMMOB 5. Ulusal Beton Kongresi*, 1-3 October, İstanbul, Türkiye.

URL-1: S. Özkan, Kanalet İnşaat - Kanalet Grubu [Online]. Available: http://www.kanalet.com.tr/firma/insaat

URL-2: News: Lağım Suyu Değil DSİ'ye Ait Sulama Kanalı - Manisa Büyükşehir Belediyesi [Online]. Available: https://www.manisa.bel.tr/Haberler/2296_lagim-suyu-degil-dsiye-ait-sulama-kanali.aspx

URL-3: News: Köyün sulama kanalı çöktü, İl Gazetesi [Online]. Available: https://www.ilgazetesi.com.tr/koyun-sulama-kanali-coktu-295475h.htm

URL-4: News: Kahramanmaraş'ta dağdan kopan kayalar 3 bin dekar araziyi sulayan kanallara zarar verdi, Anadolu Ajansı [Online]. Available: https://www.aa.com.tr/tr/asrin-felaketi/kahramanmarasta-dagdan-kopan-kayalar-3-bin-dekar-araziyi-sulayan-kanallara-zarar-verdi/2859527

URL-5: News: Su İletim ve Dağıtım Yapıları, Ankara Üniversitesi Açık Ders Malzemeleri [Online]. Available: https://acikders.ankara.edu.tr/pluginfile.php/99040/mod_resource/content/1/TSY_Blm3.pdf

URL-6: T.C. Tarım ve Orman Bakanlığı, Sulama Tesislerinde Sanat Yapıları İnşaatı Teknik Şartnamesi, 2006 [Online]. Available: https://cdniys.tarimorman.gov.tr/sulama-tesislerinde-sanat-yapilari-inşaat teknik şartnamesi.pdf

Vanani HR, Ostad-Ali-Askari K (2022). Correct path to use flumes in water resources management. *Applied Water Science*, 12(8), 187.

Xiao Z, Wu W (2022). Durability analysis of small assembled buildings in irrigation canal system. *Scientific Programming*, 2022, e2202052.

Yenigün K, Aydoğdu MH (2008). Turkiye'nin en büyük entegre su kaynakları projesi GAP'ta sulama ve drenaj sistemlerinin özet değerlendirmesi. *TMMOB*, 2, 159–174.

Yildizel SA (2020). Material properties of basalt-fiber-reinforced gypsum-based composites made with metakaolin and silica sand. *Mechanics of Composite Materials*, 56, 379-388.

Yildizel SA, Yiğit ME, Kaplan G (2017). Glass fibre reinforced concrete rebound optimization. *Computer Modeling in Engineering & Sciences*, 113(2), 203-218.

Yılmaz MC (2023). Effects of pre-cracked reinforced concrete in compression zone on prefabricated RC beam behavior. *Challenge Journal of Structural Mechanics*, 9(2) 77–83.

Yiğit ME (2019). Dalga Sediment ve Sıvılaşan Zemin İtkilerine Maruz Rıhtım Kazıklarının Dinamik Analizi. *Ph.D. thesis*, Manisa Celal Bayar University, Manisa, Türkiye.

Zhang F, Guo S, Zhang C, Guo P (2019). An interval multiobjective approach considering irrigation canal system conditions for managing irrigation water. *Journal of Cleaner Production*, 211, 293–302.

Zhang Z, Zhang HW, (2014). Solid mechanics-based Eulerian model of friction stir welding, *International Journal of Advanced Manufacturing Technology*, 72(9–12), 1647–1653.

Zwick D, Balachandar S (2020). A scalable Euler–Lagrange approach for multiphase flow simulation on spectral elements. *The International Journal of High Performance Computing Applications*, 34(3), 316-339.

Challenge Journal of Concrete Research Letters

Research Article

# Investigation of structural performances of historical building elements made with local materials using the finite element method

Saeid Zardari [a], İzzettin Kutlu [b,*], Aslan Nayeb [c]

[a] *Department of Civil Engineering, İstanbul Okan University, 34947 İstanbul, Türkiye*
[b] *Department of Architecture, Mardin Artuklu University, 47060 Mardin, Türkiye*
[c] *Department of Interior Architecture, Yeditepe University, 34755 İstanbul, Türkiye*

**ABSTRACT**

The structural performance of the materials used in historical buildings can be damaged, usually due to natural events or human-induced interference. Historical buildings in the Southeastern Anatolia Region were generally built with local materials such as stone and brick. This situation should be seen as a factor that may cause severe structural damage in buildings located on a regionally active fault line. Within the scope of the study, the materials used in the region were discussed, and a numerical model representing the behavior of the materials against an earthquake that could occur on the fault line was used. Stone, brick and concrete material definitions were made for the prototype of the arch form modeled with SAP2000, and time-history analyses were carried out separately for each material. Concrete material behaviors, frequently used in buildings constructed today, are also included in the analysis for comparison. As a result of the study, it has been observed that local materials do not have sufficient tensile strength against earthquakes compared to concrete material and that the structures may face the risk of collapse in case of seismic movements in the region.

**ARTICLE INFO**

*Article history:*
Received 27 April 2024
Revised 20 May 2024
Accepted 5 June 2024

*Keywords:*
Anatolia
Concrete
Finite element analysis
Local materials
Tension stresses



## 1. Introduction

The geographical expanse of Türkiye is situated within an active seismic belt, and historical records underscore the occurrence of numerous earthquakes in these regions throughout human history. Considering all disasters in Turkey, it is evident that natural disasters, particularly earthquakes, have a significant impact (Birinci 2023). An investigation conducted by the Turkish Statistical Institute reveals that a substantial 92.3% of the nation's territory is susceptible to seismic activity (Önal and Koçak 2005; Sayıl and Osmanşahin 2008; Öztürk 2020; Doğangün et al. 2021; Medved et al. 2021). Therefore, Türkiye consistently faces the imminent threat of earthquakes. In the pursuit of safeguarding structures against seismic impacts and enhancing their structural resilience, a paramount prerequisite involves the meticulous identification of their existing structural condition. Empirical studies have revealed that historical structures exhibit a more complex response to seismic forces when compared to contemporary buildings. Furthermore, these architectural structures demonstrate different sensitivities to seismic influences depending on the temporal context of their construction and how they have been used over time (Sezen et al. 2008; Al-Nammari and Lindell 2009; Şeker 2011; Di Ludovico et al. 2017).

Historical buildings, having survived the passage of numerous years, have been exposed to seismic activity and various external forces. Thus, the structures of historical buildings that are adversely affected by earthquakes sometimes collapse and sometimes become unusable (Camuffo et al. 2004; Sezen et al. 2008; Korkanç and Savran, 2015; Corradi et al. 2023). It is essential to identify the weak points of buildings that can be damaged in an earthquake so that historical buildings are

* *Corresponding author*. Tel.: +90-482-212-8980 ; E-mail address: izzettinkutlu@artuklu.edu.tr (İ. Kutlu)
ISSN: 2548-0928 / DOI: https://doi.org/10.20528/cjcrl.2024.03.004

minimally damaged, especially not destroyed, by earthquakes. Preserving the cultural heritage and architectural integrity of these historical structures is of paramount importance, as they represent tangible links to the past and serve as invaluable repositories of a community's identity and traditions (Örmecioğlu 2010; Ahunbay 1996; Ertaş and Bekar 2021). Therefore, it is essential to conduct seismic analyses of historical buildings that provide insights that can inform interventions aimed at preserving structural integrity without causing damage (Çırak 2011; Lacanna et al. 2020; Eriçok 2022). A large number of studies are available in the literature report applications of ambient vibration testing and operational modal analysis with multiple goals, such as damage assessment (Betti et al. 2015; Clementi et al. 2017; Alkayem et al. 2018), seismic vulnerability assessment (Bartoli et al. 2015; Erdogan 2017; İlerisoy and Soyluk), structural health assessment and monitoring (Castellazzi et al. 2012; Ramos et al. 2013; Bassoli et al. 2018), modal updating and identification (Aoki et al. 2008; Chiorino et al. 2011; Torres et al. 2017; Girardi et al. 2019; Pavlovic et al. 2019; Mertol 2023). Concurrently with the advancement of computer technology, the formulation of models for historic buildings and their structural analysis using the finite element method is progressively becoming widespread (Kutlu and Soyluk 2024).

Preserving historical buildings for future generations necessitates an initial step of comprehensive documentation. Documenting cultural assets in their current state or original form, utilizing data derived from their existing conditions, holds paramount significance (Styliadis 2007; Kutlu et al. 2023). This meticulous documentation process captures the present state and proves instrumental in discerning damages that have transpired or are likely to occur in the future. Such a proactive approach facilitates a more informed and effective strategy for preserving cultural heritage, ensuring its integrity is passed on to future generations (Durduran 2003; Donato and Giuffrida 2019). Developing conservation strategies and documentation is essential for analyzing historical buildings. Indeed, the analysis of a historical building becomes an unreliable exercise in the absence of detailed documentation. Documentation is the foundational basis, providing the essential data and details for a comprehensive structural analysis. However, documentation of historical buildings can be time-consuming. During this process, prototypes of undocumented buildings can be built, and preliminary information can be obtained. Prototypes do not contain precise information, but they can provide quick information. These models function as experimental representations, allowing for basic observations and assessments of structural behavior.

Natural stones have been esteemed for their enduring qualities and have been integral to architectural endeavors across centuries (Winkler 1997; Pereira and Marker 2016; Marzo and Neves 2020). Their incorporation into construction practices has encompassed a broad spectrum of applications, with natural stone serving as foundational elements and aesthetic enhancements alike. Notably, historical edifices stand as testaments to the extensive utilization of natural stone, where it has been employed as blocks in columns, integral components of load-bearing walls, external cladding material on facades, and flooring substrate (Kılıç 2009). The multifaceted roles that natural stones play underscore the necessity for a comprehensive assessment of their resilience against environmental factors, an examination of their technical attributes, and the formulation of judicious decisions informed by empirical data. The durability of natural stones is of paramount importance in architectural endeavors. Through the ages, architects and builders have relied on the robustness of natural stone to ensure the longevity and structural integrity of their constructions. Winkler (1997) underscores the enduring nature of natural stones, highlighting their ability to withstand the passage of time and resist deterioration caused by external forces. Moreover, Pereira and Marker (2016) emphasize the role of natural stones as a sustainable building material, owing to their innate durability and longevity, which contribute to reduced maintenance requirements and prolonged structural stability. In addition to their durability, natural stones possess a diverse array of technical properties that render them suitable for a multitude of architectural applications. Marzo and Neves (2020) delve into the intricacies of these properties, including compressive strength, porosity, thermal conductivity, and weathering resistance. Understanding these technical characteristics is imperative for architects and engineers, as it facilitates informed decision-making during the design and construction phases. For instance, the compressive strength of natural stone dictates its suitability for load-bearing applications, while its porosity influences its susceptibility to water ingress and subsequent deterioration. Wonganan et al. (2021) presents the physical and engineering properties of historical building materials and substitution materials used for the preservation of historical structures in Thailand. Eslami et al. (2012) conducted a comprehensive research study on the seismic behavior of a masonry vault structure in a historical building located in the city of Yazd. Yıldızlar et al. (2019) provides a detailed explanation of the restoration works conducted on a historical masonry building, used as a hospital building in the 1840s but now serving as the Faculty of Political Sciences of İstanbul University, based on its original geometrical and material characteristics.

Türkiye has a rich and ancient history, with numerous empires leaving deep traces and significant historical heritage across the country (Karalar and Çavuşli 2021). Anatolia has a very diverse geography in terms of natural stone. The use of these stones in architecture is quite commonly observed. However, this region is also exposed to destructive effects such as earthquakes. Türkiye, situated in a region of high seismic activity, has experienced significant consequences due to earthquakes occurring in various fault systems throughout its history (Pampal 1999; Dal Zilio and Ampuero 2023). Structural analyses are quite critical for a region that is under the earthquake effect to this extreme. This study examines the relationships established through the keywords in research literature that contains the terms "finite element analysis" and "Anatolia". The objective is to identify the common words used in this field and gain insights into the methodologies, aims and findings of the

relevant studies. The research process was conducted using the Web of Science (WoS) online database, which is utilized to monitor, analyze and access scientific research and academic publications. Specifically, the studies that have employed both "finite element analysis AND Anatolia" in their content were searched and analyzed. Accordingly, 21 studies were found in the WoS database. The VOSviewer (visualizing scientific landscapes) program was used to create bibliometric networks among these studies and visualize the keyword occurrences. The keywords that appeared at least once in the studies were shown in the program. Notably, the studies were highly related to the keywords "rock, numerical analysis, movement monitoring" (Fig. 1).

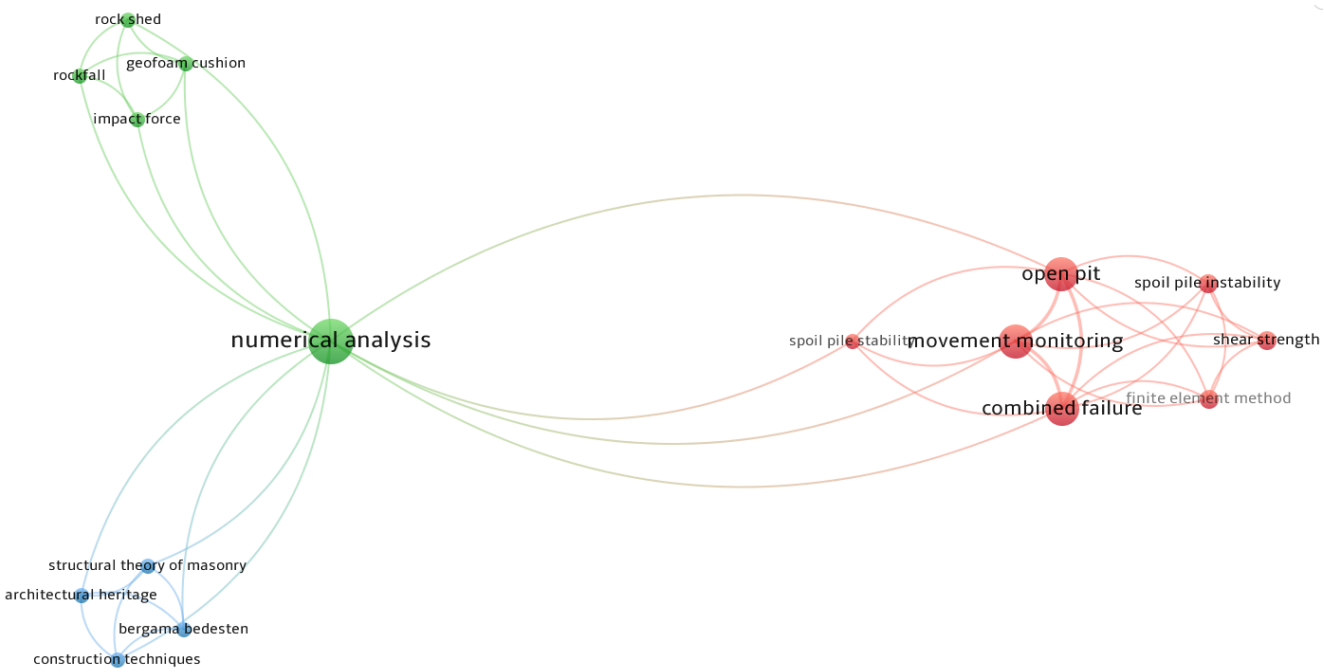


**Fig. 1.** Bibliometric analysis performed with the expression "finite element analysis and Anatolia".

Masonry structures are some of the oldest building types used throughout history. Consequently, many masonry structures hold historical significance and are still in use today (Akın and Alagöz 2024). The structural integrity of masonry systems, prevalent in historical buildings across Anatolia and particularly in the Southeastern Anatolia Region, becomes crucial in mitigating the impact of seismic events. Failure of these materials to withstand horizontal ground movements during earthquakes can lead to severe damage or collapse of historic structures. Therefore, there is a pressing need to investigate the earthquake resilience of buildings constructed with traditional materials such as stone and brick, comparing their performance to modern building materials like concrete. The primary objective of this study is to analyze the seismic behavior of structures composed of traditional materials prevalent in Anatolian historical buildings, with a particular focus on the Southeastern Anatolia Region. Mechanical properties of stone and brick, commonly utilized in these constructions, was examined in relation to their earthquake resistance. Furthermore, this research aims to juxtapose their performance against that of concrete, a staple material in contemporary construction practices. To achieve these objectives, a curvilinear structural element model, representative of arches commonly found in historical buildings, was employed. Ground motion data from four significant earthquakes in Türkiye was applied to the model, simulating seismic forces experienced by structures in the region. By subjecting these models to realistic earthquake scenarios, the study seeks to elucidate the seismic response of historical buildings along the Eastern Anatolian Fault Line. The findings of this research endeavor were expected to yield valuable insights into the seismic performance of traditional building materials prevalent in Anatolia. By discerning the strengths and limitations of stone, brick, and concrete in withstanding seismic forces, architects, engineers, and policymakers can formulate informed strategies for the preservation and retrofitting of historical structures. Ultimately, the study aims to contribute to the development of seismic-resilient building practices, safeguarding Anatolia's rich architectural heritage for future generations.

## 2. Materials and Method

The study used the finite element method to determine the changing seismic performance of local materials and compare them with concrete. Finite elements analysis, a contemporary numerical modeling method that has increased in use with the development of computer technology in recent years, is one of the most crucial modeling methods today. It is an analysis method that allows 3-dimensional static and dynamic analysis of structures; linear and non-linear analyses can be made, and the results can be displayed numerically or graphically (İmamoğlu and Çetin 2007; Demirtaş and Erkmen

2019). The finite element method of the study consists of three stages. In the first stage, the arch, whose dimensions were defined above, was modeled with the SAP2000 (Structural Analysis Program) program. In the second stage, the properties of three different materials, stone, brick, and concrete, were defined on the model created in the program. In the third stage, four ground motion records accessed on the PEER Berkeley website were applied to the arch form for each material value entered to determine the earthquake performances (Dabanlı 2008). The analysis results obtained after these stages were evaluated.

In the study, the curvilinear structural element, the arch, frequently used to pass any opening in historical buildings, is discussed, and we aim to determine the changes to be seen in the earthquake performance of the arch form with different materials. In this context, a prototype three-span arch form was created, and the material properties of the arch were defined as stone and brick materials, primarily used in the Southeastern Anatolia Region. The region is under the influence of the active East Anatolian Fault System, which poses a danger to the historical structures in the region today. Despite the intense earthquake movements on the fault in recent years, the Eastern Anatolian Fault System is thought to be in a position to cause destructive earthquakes in the next century due to the seismic gaps on the fault (Hutton 2003; Pacific Earthquake Engineering Research Center). Therefore, the studies to be carried out for the historic structures within the affected region are of great importance. Within the scope of the study, the local materials frequently encountered in the region, stone and brick, were discussed. In addition, concrete material properties are defined on the prototype arch to compare with concrete, which is one of the important building materials today. Previous experimental studies on materials from the literature were used to determine material properties. Altunışık et al. (2016) investigated the seismic behavior of the Kaya Çelebi Mosque located in Türkiye, which has been undergoing a restoration process since the 2011 Van earthquake. In their study, the researchers addressed the material mechanical properties of the historical structure. Ünay (2002), on the other hand, presented approaches regarding the general material properties of historical structures. Based on the findings of these two studies, average material mechanical properties were determined for a prototype model, and detailed information was included in the modeling process.

### *2.1. Local materials used in Southeast Anatolia*

Anatolia, positioned at the crossroads of Asia and Europe, has served as a fertile ground for the emergence of numerous civilizations since ancient times. The rich cultural legacy left behind by these civilizations not only provides valuable insights into Anatolia's past but also sheds light on various aspects of its present-day socioeconomic, cultural, and architectural landscape. Preservation efforts aimed at safeguarding Anatolia's cultural assets, spread across its seven distinct regions, play a crucial role in ensuring the transmission of this historical wealth to future generations. Among these regions, the Southeastern Anatolia Region stands out for its unique cultural heritage, shaped by the convergence of diverse civilizations over millennia. Local materials, particularly stone and brick, have played a central role in shaping the architectural identity of this region. Their abundant use in the construction of historical structures not only reflects the region's indigenous building traditions but also embodies its resilience and adaptability in the face of changing socio-political landscapes. The conservation of cultural assets in the Southeastern Anatolia Region holds profound significance, not only from a historical perspective but also in terms of fostering local identity, promoting tourism, and stimulating economic development. By preserving and showcasing the architectural marvels crafted from indigenous materials like stone and brick, the region can capitalize on its cultural heritage as a catalyst for sustainable growth and community empowerment. In essence, the discussion of local materials such as stone and brick within the context of the Southeastern Anatolia Region underscores the region's pivotal role in Anatolia's cultural narrative. By nurturing and protecting these invaluable cultural assets, Anatolia can continue to serve as a beacon of cultural heritage, inspiring curiosity, fostering understanding, and bridging the past with the present for generations to come.

Stones represent mineral formations resulting from the intricate interplay of elements within the atom-molecule-element chain, culminating in the creation of minerals, which subsequently aggregate to form stones (Yüzer et al. 2016). These mineral compositions, shaped by geological processes over eons, have been integral to human existence since antiquity, enduring through the passage of time and the advancements of technology. Despite the evolution of civilization and the advent of modern materials, natural stones persist as essential elements in various facets of human life. Türkiye stands out as a fortunate nation endowed with abundant natural stone resources, boasting remarkable reserves and diversity (Taşlıgıl and Şahin 2016). This geological wealth spans a spectrum of stone types, including marble, granite, limestone, travertine, and many others, each characterized by distinct aesthetic, structural, and functional properties. The country's geological diversity, coupled with its strategic location bridging continents, positions Türkiye as a global hub for natural stone extraction, processing, and trade.

Türkiye has proven itself in this market, especially in production and export in recent years. At the same time, Türkiye has a special place in the sector with its unique stones and geographical location (Erkanol and Aydındağ 2013). In addition to all these positive aspects, unfortunately, there are still many shortcomings. Historical buildings, in which Türkiye's natural stone existence is shaped as a cultural and architectural heritage, are faced with many dangers today. When stone structures are examined, we can see that weathering occurs for many reasons. Stones are often exposed to deterioration due to environmental and time-dependent factors. Natural stones weaken over time with these effects and lose their physical-mechanical properties (Hasbay and Hattap

2017). It is essential to know the factors that cause deterioration in stones, to take precautions accordingly to prevent the deterioration of stones and to transfer the structures from generation to generation.

Natural stones, commonly used in some cities consisting of common areas where people live together, give this city a separate visual identity. For example, 'Bakirkoy Küfeki Stones and Marmara Island marbles' used in historical buildings in İstanbul, 'andesites' in early republican period buildings in Ankara, 'basalts' in Diyarbakir, and easily processed 'limestones' in Urfa and Mardin can be shown among them (Yüzer et al. 2016; Kazancı and Gürbüz 2017). Another material used in the region is clay, the raw material of brick. It is possible to divide the materials made of clay into two as baked and unbaked. The leading unbaked material is mud-brick. Bricks and tiles can be given as examples of baked materials. The production method of brick and tile is the same, only the molding systems are different (Şimşek 2003). Regional conditions are important in the use of brick. Therefore, structures made of stone draw attention due to the density of stone resources in Anatolia, Caucasus, Crete, and Cyprus. Due to the limited availability of stone in Mesopotamia, Iran, Central Asia, and Egypt, it was replaced by brick. In these regions, stone was only used to reinforce the brickwork (Bakırer 1981; Eroğlu and Akyol 2017).

### *2.2. Modeling of materials using the prototype finite element method*

In the study, the arch, one of the most important elements of historical buildings, is handled as four spans. The external dimensions of the created model are 15.0 x 1.0, the arch height is 4 meters, and the total height is 5 meters. The arch piers are arranged as 1 m each, the middle openings 3 m, and the openings at the corners 2 m (Fig. 2). The study's primary purpose is to identify the differences between the materials. For this reason, this data was not included in the analysis process, so that the results obtained from the created model would be independent of the region and soil characteristics.

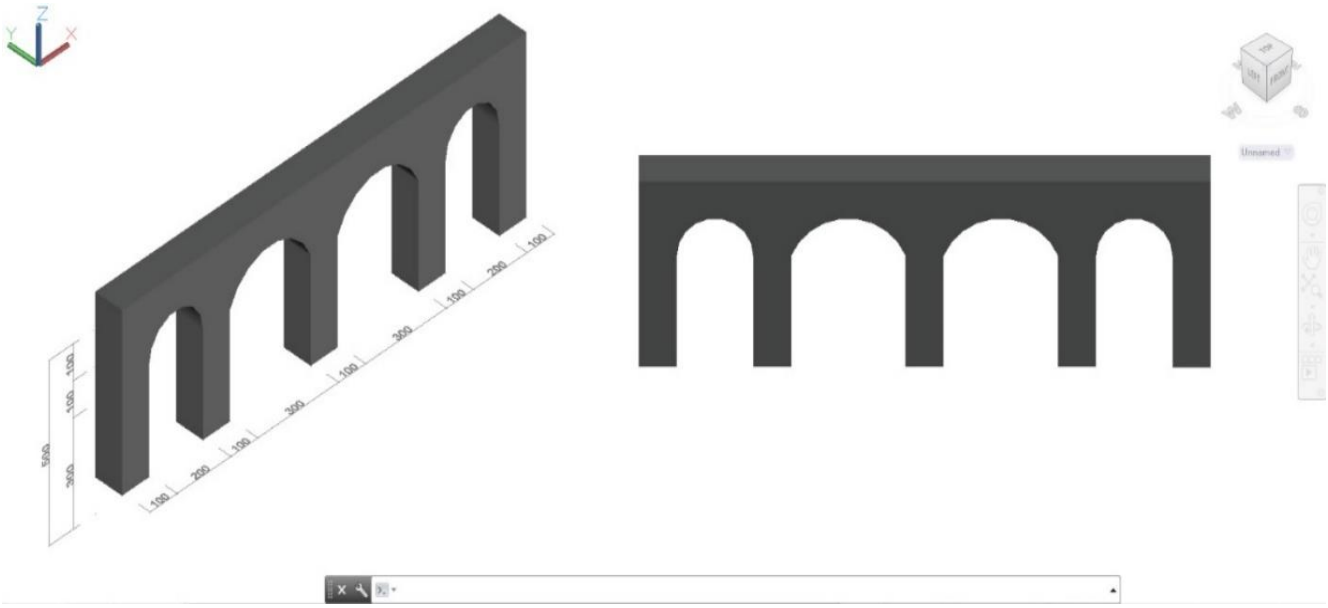

**Fig. 2.** Prototype model.

The mechanical properties of the materials used in the modeled prototype arch are given Table 1, and for this purpose, a finite element model of the prototype model was created in line with the model preparation features and rules of the SAP2000 software.

Model creation and calculation values are given below:

- The building's masonry walls and vault cover were modeled with SHELL elements.
- The relationship of the building with the ground was defined as fixed support.
- The model to be analyzed was prepared with 304 nodes and 95 SHELL elements (Fig. 3).
- Linear elastic calculation methods are also sufficient to comment on the modeled structural elements' general structural and seismic behavior, such as arches. In cases where more detailed results are desired, nonlinear methods and experimental studies can also be evaluated. In the study, it was accepted that the materials defined in the model showed linear elastic behavior together with the mortar.
- The material properties used in the analysis for the masonry prototype model were produced as a result of previous studies for similar structures in the region and are given in Table 1 above.
- In order to interpret the earthquake resistance data obtained as a result of the analysis, the resulting stresses were compared with the safety stresses of the material used in the building. The safety stresses of materials in the literature were used as mentioned (Altunışık et al. 2016; Ünay 2002). C25/30 was used for concrete, and the properties were implemented according to TS 500. The accepted safety stresses for the stone, brick and concrete used in the prototype model were presented in Table 2.

**Table 1.** Mechanical properties of the materials used in the arch during the analysis process and finite element model of prototype building (Altunışık et al. 2016; Ünay 2002).

| Structural components | Modulus of elasticity (N/m²) | Density (kg/m³) | Poisson's ratio |
|---|---|---|---|
| Stone wall (with mortar) | $4.50 \cdot 10^8$ | 2400 | 0.200 |
| Brick | $1.20 \cdot 10^9$ | 2400 | 0.200 |

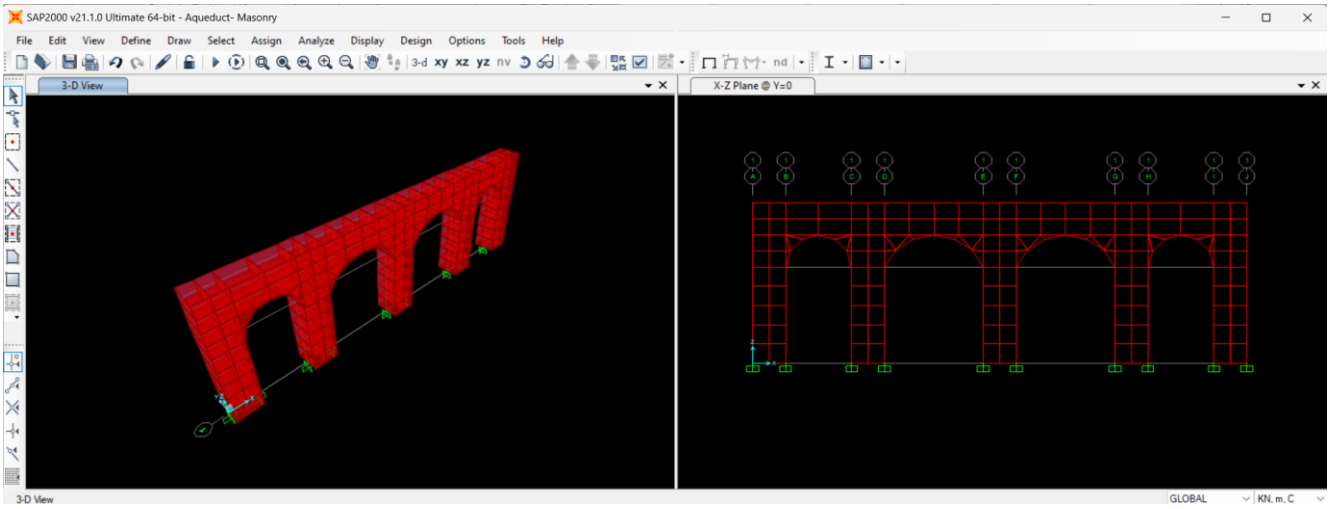


**Fig. 3.** Finite element model view of the prototype in SAP2000.

**Table 2.** The accepted safety stresses for the materials used in the prototype model.

| Materials | Pressure safety stresses (MPa) | Tension safety stresses (MPa) |
|---|---|---|
| Stone wall (with mortar) | 0.90 | 0.135 |
| Brick | 2.40 | 0.360 |
| Concrete | 25.0 | 1.800 |

With numerical modeling, analyses are prepared to observe the reaction of the whole or some parts of the structure under different loads or physical effects. This part of the study aims to apply four different ground motion records on the prototype model, the dimensions, and the plan mentioned above and to analyze the response of the structural element to these earthquake loads. Earthquake records were taken from different stations as indicated in Table 3. The first of these records was the earthquake that took place in Erzincan in 1992 with a magnitude of Mw=6.69; the second and third earthquakes occurred in Kocaeli in 1999 with Mw=7.51; the fourth is the earthquake of Mw=7.14, which took place in Düzce in 1999 (Ministry of Interior, Disaster and Emergency Management Presidency, Türkiye).

**Table 3.** Characteristics of ground motion records (Peak Ground Acceleration – PGA).

| No. | Record ID | Event | Year | Station | Magnitude | Fault distance (km) | PGA-1[1] (g) | PGA-1[2] (g) |
|---|---|---|---|---|---|---|---|---|
| 1 | 821 | Erzincan, Türkiye | 1992 | Erzincan | 6.69 | 0.00 | 0.496 | 0.386 |
| 2 | 1166 | Kocaeli, Türkiye | 1999 | İznik | 7.51 | 30.73 | 0.124 | 0.090 |
| 3 | 1158 | Kocaeli, Türkiye | 1999 | Düzce | 7.51 | 13.60 | 0.312 | 0.364 |
| 4 | 1605 | Düzce, Türkiye | 1999 | Düzce | 7.14 | 0.00 | 0.404 | 0.515 |

## 3. Findings

First of all, the behavior under modal analysis was examined to analyze the structure's behavior under dynamic loads, independent from the region and earthquake, only depending on its system. Mode 1 and Mode 3 shapes that dominate in *Y* and *X* directions are shown in Fig. 4(a-b), and the period values resulting from the modal analysis are given in Table 4.

**Table 4.** Period values of the dominant Mode 1 and Mode 3 of the prototype model.

| Materials | | Mode 1 | Mode 2 | Mode 3 |
|---|---|---|---|---|
| Stone | T(s) | 0.56 | 0.41 | 0.26 |
| Brick | T(s) | 0.34 | 0.15 | 0.15 |
| Concrete | T(s) | 0.07 | 0.032 | 0.032 |

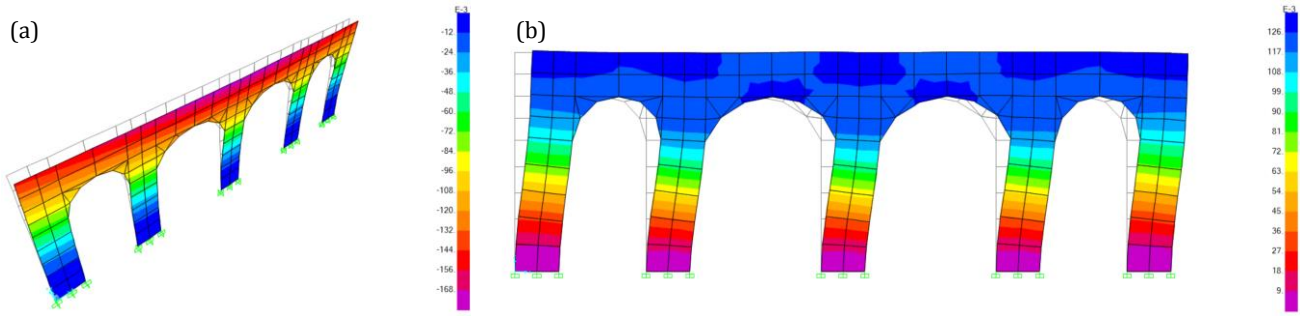


**Fig. 4.** Modal analysis: (a) Mode 1 translation is in the *Y* direction; (b) Mode 3 translation is in the *X* direction.

Four different ground motion recordings were applied to the arch from which the prototype model was created. For each earthquake record, the behaviors of the arch element, whose stone, brick, and concrete materials were defined, were compared. As the dynamic response of the arch, the displacements and the maximum compressive and tensile stresses in the materials are investigated. When the earthquake acceleration records are applied to the model and the stresses occurring in the structure are compared, the most significant stress was obtained from the Erzincan earthquake acceleration record. *X* and *Y* direction compressive stress values obtained from recordings applied to the prototype arch for all three materials are shown in Figs. 5(a-b), 6(a-b), and 7(a-b). Time-history analysis results are given in Table 5.

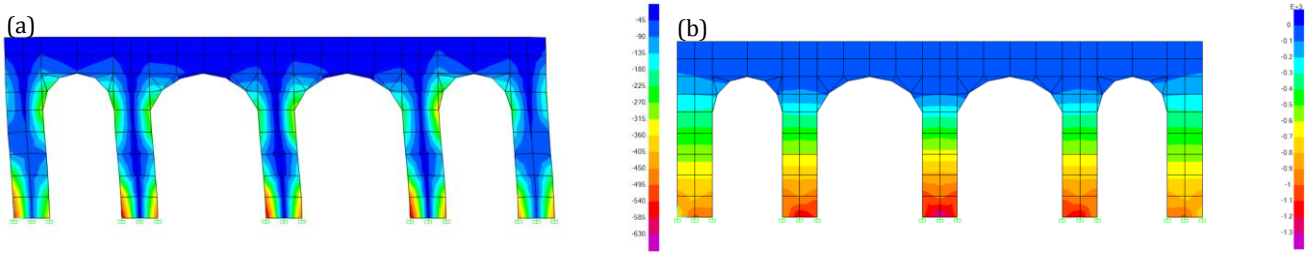


**Fig. 5.** Compressive stresses obtained from the Erzincan earthquake analyses for the stone arc: (a) *X* direction; (b) *Y* direction.

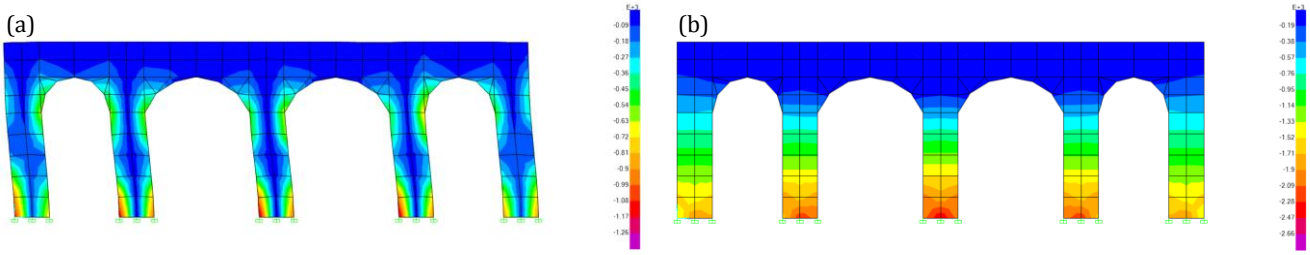


**Fig. 6.** Compressive stresses obtained from the Erzincan earthquake analyses for the brick arc: (a) *X* direction; (b) *Y* direction.

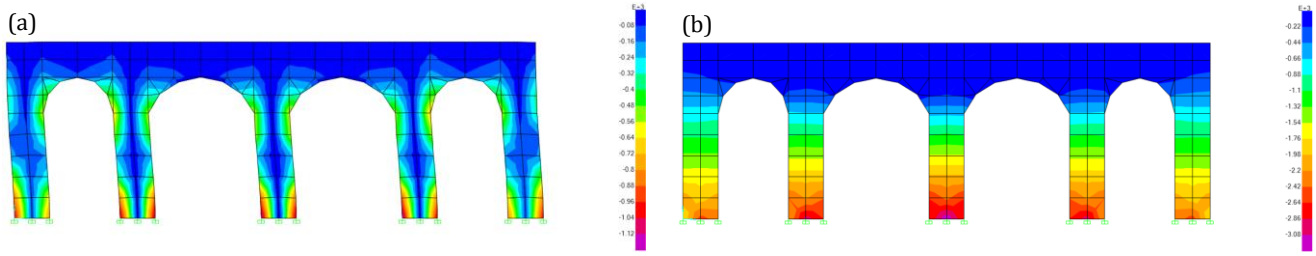


**Fig. 7.** Compressive stresses obtained from the Erzincan earthquake analyses for the concrete arc: (a) *X* direction; (b) *Y* direction.

The result of the earthquake code 821 (Erzincan) was applied in the *X* direction. The analysis values were provided in the Table 5. For stone material, the maximum compressive stress value is 0.652 MPa, and the maximum tensile stress value is 0.650 MPa. The maximum compressive stress value for brick material is 1.300 MPa, and the maximum tensile stress value is 1.300 MPa. The maximum compressive stress value for the concrete material was 1.252 MPa, and the maximum tensile stress value was 1.250 MPa.

**Table 5.** Maximum compression stresses and maximum tensile stresses (MPa).

| | | | Stone | Brick | Concrete |
|---|---|---|---|---|---|
| Maximum compression stresses | Erzincan 821 | Ex | 0.652 | 1.300 | 1.252 |
| | | Ey | 1.423 | 2.544 | 3.292 |
| | Kocaeli 1166 | Ex | 0.526 | 0.475 | 0.329 |
| | | Ey | 0.379 | 0.753 | 1.029 |
| | Kocaeli 1158 | Ex | 0.376 | 0.691 | 0.770 |
| | | Ey | 0.489 | 1.795 | 3.555 |
| | Düzce 1605 | Ex | 0.450 | 1.416 | 0.906 |
| | | Ey | 0.654 | 1.847 | 5.350 |
| Maximum stresses | Erzincan 821 | Ex | 0.650 | 1.300 | 1.250 |
| | | Ey | 1.397 | 2.807 | 2.138 |
| | Kocaeli 1166 | Ex | 0.526 | 0.474 | 0.329 |
| | | Ey | 0.330 | 0.771 | 0.865 |
| | Kocaeli 1158 | Ex | 0.375 | 0.690 | 0.770 |
| | | Ey | 0.619 | 1.609 | 4.986 |
| | Düzce 1605 | Ex | 0.450 | 1.416 | 0.906 |
| | | Ey | 1.099 | 1.408 | 5.674 |

Maximum displacements were given in Table 6. In SAP2000, U1 and U2 typically represent the displacement components in the global *X* and *Y* directions, respectively, for a structural analysis model. When you perform a structural analysis using SAP2000, the software calculates various results to help you understand how the structure behaves under different loading conditions. Displacement results, represented by U1 and U2, provide information about how much the structure moves or deforms in the *X* and *Y* directions, respectively, due to applied loads. As can be seen from the results, the maximum displacement for the stone material was 38.9 mm displacement under the effect of the acceleration in the *Y* direction of the Erzincan earthquake. This value was determined as 29.3 mm for brick material and 1.33 mm for concrete material.

**Table 6.** Maximum displacements (mm).

| | Stone | | Brick | | Concrete | |
|---|---|---|---|---|---|---|
| | U1 | U2 | U1 | U2 | U1 | U2 |
| Erzincan - 821 | 8.27 | 38.9 | 6.18 | 29.30 | 0.22 | 1.33 |
| Kocaeli - 1166 | 6.60 | 10.3 | 2.20 | 8.01 | 0.061 | 0.41 |
| Kocaeli - 1158 | 4.70 | 17.0 | 3.28 | 18.70 | 0.142 | 2.02 |
| Düzce -1605 | 5.70 | 30.0 | 6.70 | 19.40 | 0.15 | 2.30 |

## 4. Evaluation

Finite element analysis (FEA) was conducted utilizing linear elastic material properties to investigate the behavior of a modeled arch element subjected to four distinct ground motion scenarios. Through meticulous calculations, comprehensive insights were gained into the performance of the arch form constructed from three different materials in response to seismic forces and stress effects anticipated during an earthquake event. The utilization of FEA enabled the simulation of complex structural behaviors under varying seismic conditions, providing a rigorous assessment of the arch element's response to dynamic loading. By employing linear elastic material properties, the analysis accounted for the linear relationship between stress and strain within the materials, allowing for a precise evaluation of structural performance within the elastic deformation regime. The examination encompassed the evaluation of displacement patterns, stress distributions,

and deformation mechanisms exhibited by the arch element under different ground motion excitations. Through systematic analysis, notable distinctions in the seismic response of the arch form constructed from different materials were elucidated, shedding light on their respective capacities to withstand earthquake-induced forces. The outcomes of the study unveiled critical insights into the seismic resilience of the arch element modeled with various materials, delineating their abilities to resist external loads and endure stress effects arising from seismic activity.

When the compressive stresses in the analysis results are examined, the stone arch element is durable for all three earthquake records, but the maximum compressive stress of the stone was obtained as 1.423 MPa under the effect of the Erzincan earthquake in the *Y* direction. Since the obtained compressive stress is higher than the value of 0.9 MPa, which is accepted in the material properties, the stone material could not show sufficient compressive strength during the Erzincan earthquake. The brick arch element is also durable for all three earthquake records, but the maximum compressive stress of the brick was obtained as 2.544 MPa under the effect of the Erzincan earthquake in the *Y* direction. Since the obtained compressive stress is higher than 2.4 MPa, which is accepted in the material properties, the brick material could not show sufficient compressive strength during the Erzincan earthquake. Concrete material showed sufficient compressive strength against all four earthquake records. Therefore, brick and stone could not show sufficient compressive strength against the *Y* direction effect of the Erzincan record.

When the tensile stresses were examined, the stone and brick arch elements did not show sufficient tensile strength for all four earthquake records. Concrete material showed sufficient tensile strength in the X direction earthquake effects but could not show sufficient tensile strength in the Y direction effects of the Erzincan, 1158-Kocaeli, and Düzce records. Therefore, it has been observed that the tensile strength of stone and brick materials is insufficient, and concrete has sufficient strength.

## 5. Conclusions

Determining the behavior of the structural elements that make up the historical structures under the influence of earthquakes is very important for protecting these structures. In this study, using the finite element method, an arch model was created in the SAP2000 program, and ground motion records of 4 different earthquakes in our country were examined by applying them to time-history analysis. During the examination, stone and brick, which are frequently encountered as local materials in the historical structures of the Southeast Anatolian Region, which is under the influence of the Eastern Anatolian Fault System, and concrete materials that are frequently used in today's contemporary architecture are defined separately for the arch, after the ground motion records applied to the arch elements that emerged as a result of the material definitions, the displacement and stress values were discussed. The results were compared according to the material behavior. In the results of four different ground motion records applied separately for each material, generally, the highest stress values were observed in the Erzincan earthquake, with a magnitude of 6.9 in 1992.

When the data was considered numerically;

- It was observed that the compressive stress of the stone arch element exceeded the safety stress only in the *Y* direction effect of the Erzincan earthquake. While the same is true for the brick arch element, the concrete showed sufficient compressive strength against all four earthquake records and did not exceed the safety stress. Therefore, in compressive stresses, it can be concluded that concrete is the safest material against all four records. It is seen that when the stone and brick exceed the safety stress, the concrete does not even reach approximately 20% of its safety strength.
- While stone and brick arch elements could not show sufficient tensile strength for all four earthquake records in both directions, concrete showed sufficient tensile strength in *X* direction records, but it could not show sufficient tensile strength in the Erzincan, 1158 Kocaeli and Düzce records in the *Y* direction. Since concrete cannot show sufficient resistance to tensile strength as a material property, it is reinforced with reinforcements today.
- While it has approximately sufficient strength in the compressive stress of stone and brick, which is frequently used as local material, it has low strength in tensile stress. Tensile strengths may vary depending on the properties of the mortar used as binding material. Therefore, if a mortar with high binding properties is used, an increase in the safety tensile strength can be observed.
- Since stone and brick behave more flexibly than concrete, they showed more displacement under the effect of ground motion records applied. In terms of material properties, concrete has a higher modulus of elasticity and behaves more rigidly than other materials. Therefore, in the analyses made, the concrete showed less displacement. When the periods of the structure in the modes are examined, the lowest period belongs to the concrete structural element, confirming that the concrete has shown a rigid behavior.
- In the event of an earthquake with an earthquake acceleration record similar to the Erzincan earthquake in the Eastern Anatolian Fault System, it can be predicted that the historical buildings with stone and brick arches in the region cannot provide sufficient compressive and tensile strengths where there is a risk of damage.

The evaluation of the obtained results has revealed that the local materials used in the arches, which are commonly found in historical buildings, may not exhibit sufficient resistance against seismic forces compared to contemporary building materials such as concrete. This finding is particularly significant, as historical structures often rely on traditional construction techniques and local materials, which may not have

been designed with modern earthquake engineering principles in mind.

The time-history analyses conducted within the scope of the study provide valuable insights into the dynamic behavior of these historical structures under earthquake loading. These advanced analytical techniques allow for a more comprehensive understanding of the structural response, including the identification of critical failure modes and the quantification of the seismic performance. The results of these analyses can serve as a foundation for future studies, informing the development of more effective seismic assessment and retrofitting strategies for historical buildings. To further expand the knowledge in this field, it is essential to carry out similar studies on a wider range of historical buildings, encompassing different construction materials, structural systems, and architectural styles. This diversity of case studies would enable researchers to identify patterns, correlations, and underlying factors that influence the seismic performance of these structures. Additionally, the integration of advanced computational modeling and experimental validation could provide a more robust and reliable framework for assessing the seismic vulnerability of historical buildings.

Furthermore, future studies may explore the incorporation of traditional construction techniques and local materials into modern seismic design approaches. By understanding the inherent strengths and weaknesses of these traditional systems, researchers can work towards developing innovative retrofitting solutions that preserve the cultural heritage and architectural integrity of historical structures while enhancing their seismic resilience. This multidisciplinary approach, combining historical knowledge, structural engineering principles, and sustainable design, could pave the way for more effective and holistic preservation strategies for our architectural legacy.

***Acknowledgements***

*None declared.*

***Funding***

*The authors received no financial support for the research, authorship, and/or publication of this manuscript.*

***Conflict of Interest***

*The authors declared no potential conflicts of interest with respect to the research, authorship, and/or publication of this manuscript.*

***Author Contributions***

*All of the authors made substantial contributions to conception and design, or acquisition of data, or analysis and interpretation of data; were involved in drafting the manuscript or revising it critically for important intellectual content; and gave final approval of the version to be published.*

***Data Availability***

*The datasets created and/or analyzed during the current study are not publicly available, but are available from the corresponding author upon reasonable request.*

## REFERENCES

Ahunbay Z (1996). Tarihi çevre koruma ve restorasyon. YEM Publishing, İstanbul.

Akın S, Alagöz A (2024). Structural behavior of historical Obruk Inn under different earthquakes. *Challenge Journal of Structural Mechanics*, 10(1), 21-33.

Alkayem NF, Cao M, Zhang Y, Bayat M, Su Z (2018). Structural damage detection using finite element model updating with evolutionary algorithms: a survey. *Neural Computing and Applications*, 30, 389–411.

Al-Nammari FM, Lindell MK (2009). Earthquake recovery of historic buildings: exploring cost and time needs. *Disasters*, 33(3), 457-481.

Altunışık AC, Bayraktar A, Genç A (2016). A study on seismic behaviour of masonry mosques after restoration. *Earthquakes and Structures*, 10(6), 1331-1346.

Aoki T, Sabia D, Rivella D (2008). Influence of experimental data and FE model on updating results of a brick chimney. *Advances in Engineering Software*, 39, 327–335.

Bakırer Ö (1981). Selçuklu Öncesi ve Selçuklu Dönemi Anadolu Mimarisinde Tuğla Kullanımı (The Use of Brick in Pre-Seljuk and Seljuk Period Anatolian Architecture). *Ph.D. thesis,* Middle East Technical University, Ankara, Türkiye.

Bartoli G, Betti M, Borri C (2015). Numerical modelling of the structural behaviour of Brunelleschi's dome of Santa Maria del Fiore. *International Journal of Architectural Heritage*, 9, 408–429.

Bassoli E, Vincenzi L, D'Altri AM, de Miranda S, Forghieri M, Castellazzi G (2018). Ambient vibration-based finite element model updating of an earthquake-damaged masonry tower. *Structural Control and Health Monitoring*, 25(5), e2150.

Betti M, Facchini L, Biagini P (2015). Damage detection on a three-storey steel frame using artificial neural networks and genetic algorithms. *Meccanica*, 50, 875–886.

Birinci F (2023). Turkey's disaster and emergency profile: Settlement information and analysis of earthquake parameters. *Challenge Journal of Structural Mechanics*, 9(2), 55-67.

Camuffo D, Pagan E, Bernardi A, Becherini F (2004). The impact of heating, lighting and people in re-using historical buildings: a case study. *Journal of Cultural Heritage*, 5(4), 409-416.

Castellazzi G, de Miranda S, Mazzotti C (2012). Finite element modelling tuned on experimental testing for the structural health assessment of an ancient masonry arch bridge. *Mathematical Problems in Engineering*, 2012, 495019.

Chiorino MA, Ceravolo R, Spadafor A, Zanotti Fragonara L, Abbiati G (2011). Dynamic characterization of complex masonry structures: the sanctuary of vicoforte. *International Journal of Architectural Heritage*, 5, 296–314.

Clementi F, Pierdicca A, Formisano A, Catinari F, Lenci S (2017). Numerical model upgrading of a historical masonry building damaged during the 2016 Italian earthquakes: the case study of the Podestà palace in Montelupone (Italy). *Journal of Civil Structural Health Monitoring*, 7, 703–717.

Corradi M, Mustafaraj E, Speranzini E (2023). Sustainability considerations in remediation, retrofit, and seismic upgrading of historic masonry structures. *Environmental Science and Pollution Research*, 30(10), 25274-25286.

Çırak İF (2011). Yığma yapılarda oluşan hasarlar, nedenleri ve öneriler (Damages observed in masonry structures, causes and recommendations). *Süleyman Demirel University International Technologic Science*, 3(2), 55-60.

Dabanlı Ö (2008). Tarihi Yığma Yapıların Deprem Performansının Belirlenmesi (Determination of the earthquake performance of historical masonry structures). *M.Sc. thesis*, İstanbul Technical University, İstanbul, Türkiye.

Dal Zilio L, Ampuero JP (2023). Earthquake doublet in Turkey and Syria. *Communications Earth & Environment*, 4(1), 71.

Demirtaş R, Erkmen C (2019). Doğu Anadolu Fay Sistemi deprem etkinliği-gelecek deprem potansiyeli (East Anatolian Fault System seismic activity-future earthquake potential). https://doi.org/10.13140/RG.2.2.24235.49449 [accessed 26-12-2024].

Di Ludovico M, Prota A, Moroni C, Manfredi G, Dolce M (2017). Reconstruction process of damaged residential buildings outside historical centres after the L'Aquila earthquake: part I—"light damage" reconstruction. *Bulletin of Earthquake Engineering*, 15, 667-692.

Doğangün A, Yön B, Onat O, Emin Öncü M, Sağıroğlu S (2021). Seismicity of East Anatolian of Turkey and failures of infill walls induced by major earthquakes. *Journal of Earthquake and Tsunami*, 15(04), 2150017.

Donato E, Giuffrida D (2019). Combined methodologies for the survey and documentation of historical buildings: The Castle of Scalea (CS, Italy). *Heritage*, 2(3), 2384-2397.

Durduran Z (2003). Tarihi Eserlerin fotogrametrik olarak belgelenmesi ve coğrafi bilgi sistemine aktarılması (Documentation and analysis of cultural heritage by photogrammetric methods and GIS). *Ph.D. thesis*, İstanbul Technical University, İstanbul, Türkiye.

Erdogan YS (2017). Discrete and continuous finite element models and their calibration via vibration and material tests for the seismic assessment of masonry structures. *International Journal of Architectural Heritage*, 11, 1026–1045.

Eriçok AK (2022). Bitlis kent merkezinde kültür varlıklarına yönelik tehlikelerin değerlendirilmesi ve koruma önerileri (An Evaluation of the Risks of Damage to Cultural Assets in Bitlis City Center and Protection Suggestions). *Yuzuncu Yil University Journal of the Institute of Natural and Applied Sciences*, 27(1), 121-139.

Erkanol D, Aydındağ A (2013). Türkiye geneli doğal taş potansiyel alanlarının belirlenmesi projesi (Project for determination of natural stone potential areas throughout Turkey). https://www.mta.gov.tr/v3.0/sayfalar/hizmetler/kutuphane/ekonomi-bultenleri/2013_16/147.pdf [accessed 18-12-2024].

Eroğlu M, Akyol AA (2017). Antik yapı malzemesi olarak tuğla ve kiremit: Boğsak adası Bizans yerleşimi örneklemi (Brick and tile as ancient building materials: A sample of the Byzantine settlement of Boğsak Island). *Sanat ve Tasarım Dergisi*, (20), 141-162.

Ertaş BS, Bekar İ (2020). Functional Performance after Re-use in Traditional Houses. *In: Christov I, Krystev V, Efe R, Gad AA, editors. Advances in Scientific Research: Engineering and Architecture.* St. Kliment Ohridski University Press, Sofia, 418-428.

Eslami A, Ronagh HR, Mahini SS, Morshed R (2012). Experimental investigation and nonlinear FE analysis of historical masonry buildings–A case study. *Construction and Building Materials*, 35, 251-260.

Girardi M, Padovani C, Pellegrini D, Robol L (2019). A model updating procedure to enhance structural analysis in the FE code NOSA-ITACA. *Journal of Performance of Constructed Facilities*, 33, e04019041.

Hasbay U, Hattap S (2017). Doğal taşlardaki bozunma (ayrışma) türleri ve nedenleri (Types of and reasons for degradation in natural stones). *Munzur Üniversitesi Bilim ve Gençlik Dergisi*, 5(1), 23-45.

Hutton DV (2003). Fundamentals of finite element analysis. McGraw-Hill Education, New York, USA.

İlerisoy ZY, Soyluk A (2012). Impact of shallow earthquakes on the Sehzade Mehmet Mosque. *Gradevinar*, 64(9).

İmamoğlu MŞ, Çetin E (2007). Güneydoğu Anadolu Bölgesi ve yakın yöresinin depremselliği (The seismicity of Southeast Anatolian and vicinity). *Journal of Dicle University Ziya Gökalp Faculty of Education*, (9), 93-103.

Karalar M, Çavuşli M (2021). Strengthening and performance assessing historical cinema hall balcony according to new Turkish Earthquake Code. *Challenge Journal of Structural Mechanics*, 7(1), 27-41.

Kazancı N, Gürbüz A (20014). Jeolojik miras nitelikli Türkiye doğal taşları (Geological heritage qualified natural stones of Turkey). *Geological Bulletin of Turkey*, 57(1), 19-44.

Kılıç İ (2009). Edirne (Keşan) bölgesi kumtaşlarının yapı taşı olarak kullanılabilirliği (The usability of Edirne (Kesan) region sandstones as building stone). *Ph.D. thesis*, Trakya University, Edirne, Türkiye.

Korkanç M, Savran A (2015). Impact of the surface roughness of stones used in historical buildings on biodeterioration. *Construction and Building Materials*, 80, 279-294.

Kutlu I, Soyluk A (2024). A comparative approach to using photogrammetry in the structural analysis of historical buildings. *Ain Shams Engineering Journal*, 15(1), 102298.

Kutlu I, Soyluk A, Aydin S (2023). A review of the usability of photogrammetry technique for studying the structural behavior of historical buildings. *Selcuk University Journal of Engineering Sciences*, 22(1), 43-48.

Lacanna G, Betti M, Ripepe M, Bartoli G (2020). Dynamic identification as a tool to constrain numerical models for structural analysis of historical buildings. *Frontiers in Built Environment*, 6, 40.

Marzo C, Neves R (2020). Stereotomic design: The use of stone in contemporary architecture. *Key Engineering Materials*, 848, 165-173.

Medved I, Polat G, Koulakov I (2021). Crustal structure of the Eastern Anatolia Region (Turkey) based on seismic tomography. *Geosciences*, 11(2), 91.

Mertol H (2023). Failure of Gedikbulak K-12 School Building on October 23, 2011, in Van, Turkey Earthquake. *Yuzuncu Yil University Journal of the Institute of Natural and Applied Sciences*, 28(2), 544-560.

Ministry of Interior, Disaster and Emergency Management Presidency, Türkiye. https://en.afad.gov.tr [accessed 22-12-2023].

Önal MM, Koçak A (2005). Yığma yapı hasarları ve onarım ve güçlendirme yöntemlerinin ayrıntıları (Details of masonry damage and repair and strengthening methods). *Proceedings of the Antalya Yöresinin İnşaat Mühendisliği Sorunları Kongresi*, Antalya, Türkiye, 93-108.

Örmecioğlu HT (2010). Tarihi yapıların yapısal güçlendirilmesinde ana ilkeler ve yaklaşımlar. *Politeknik Dergisi*, 13(3), 233-237.

Öztürk S (2020). A study on the variations of recent seismicity in and around the Central Anatolian region of Turkey. *Physics of the Earth and Planetary Interiors*, 301, 106453.

Pacific Earthquake Engineering Research Center. https://ngawest2.berkeley.edu [accessed 21-12-2023].

Pampal S (1999). Depremler (Earthquakes). Alfa Publishing, İstanbul, Türkiye.

Ramos LF, Aguilar R, Lourenco PB, Moreira S (2013). Dynamic structural health monitoring of Saint Torcato church. *Mechanical Systems and Signal Processing*, 35, 1–15.

Pavlovic M, Trevisani S, Cecchi A (2019). A procedure for the structural identification of masonry towers. *Journal of Nondestructive Evaluation*, 38, 38.

Pereira D, Marker B (2016). The value of original natural stone in the context of architectural heritage. *Geosciences*, 6(1), 13.

Sayıl N, Osmanşahin İ (2008). An investigation of seismicity for western Anatolia. *Natural Hazards*, 44, 51-64.

Sezen H, Acar R, Dogangun A, Livaoglu R (2008). Dynamic analysis and seismic performance of reinforced concrete minarets. *Engineering Structures*, 30(8), 2253-2264.

Styliadis AD (2007). Digital documentation of historical buildings with 3-D modeling functionality. *Automation in Construction*, 16(4), 498-510.

Şeker BŞ (2011). Mimar Sinan Camilerinin Statik ve Dinamik Yükler Etkisinde Davranışlarının İncelenmesi (Investigation of Behaviour of Architect Sinan's Mosques under Static and Dynamic Loads). *Ph.D. thesis*, Karadeniz Technical University, Trabzon, Türkiye.

Şimşek O (2003). Yapı malzemesi (Builging materials). Beta Publishing, İstanbul, Türkiye.

Taşlıgil N, Şahin G (2016). Yapı malzemesi olarak kullanılan Türkiye doğal taşların iktisadi coğrafya odağında analizi (Analysis of Turkish natural stones used as building materials on the basis of economic geography). *Marmara Geographical Review*, (33), 607-640.

Torres W, Almazan JL, Sandoval C, Boroschek R (2017). Operational modal analysis and FE model updating of the metropolitan cathedral of Santiago, Chile. *Engineering Structures*, 143, 169–188.

Ünay Aİ (2002). Tarihi yapıların depreme dayanımı. METU Publishing, Ankara, Türkiye.

Winkler E (1997). Stone in Architecture: Properties, Durability. Springer Science & Business Media, Berlin, Germany.

Wonganan N, Athisakul C, Tanchirapat W, Sahamitmongkol R, Leelataviwat S (2021). Ancient materials and substitution materials used in Thai historical masonry structure preservation. *Journal of Renewable Materials*, 9(2), 179-204.

Yildizlar B, Sayin B, Akcay C (2019). A case study on the restoration of a historical masonry building based on field studies and laboratory analyses. *International Journal of Architectural Heritage*, 14(9), 1341-1359.

Yüzer E, Güngör Y, Aydoğan S (2016). Doğal Taşın Öyküsü (The Story of Natural Stone). Kare Publishing, İstanbul, Türkiye.